Big Data, Alternative Payment Data, and Artificial Intelligence in Japan's Payment System:

Thierry U. KAME BABILLA
University of Yaounde II and Euro Area Business Cycle Network

Abstract

This paper develops an open-economy Dynamic Stochastic General Equilibrium (DSGE) model that uses big data, alternative payment data, and artificial intelligence (AI) methods to analyze Japan's payment system. We augment a New Keynesian framework with (i) an AI-enhanced payment sector with endogenous fintech adoption, (ii) high-frequency transaction records from the Zengin system, QR-code platforms, and card networks, (iii) machine-learning measurement of latent payment frictions, and (iv) a central bank digital currency (CBDC) as an additional monetary instrument. Estimated by Bayesian methods on monthly data for 2000M1–2025M12, the model identifies substantial heterogeneity in the pass-through of monetary policy across payment media. AI-driven fintech adoption amplifies the domestic credit channel and lowers cross-border transaction costs. In the post-2022 sub-sample the Bank of Japan's (BOJ) Taylor-rule inflation coefficient rises to 1.88 and its fintech coefficient to 0.14. A digital yen reduces steady-state transaction costs by 15–22 basis points, and the COVID payment shift amplifies cash displacement by about 33% relative to the baseline.

JEL Classification: E42, E47, E52, F41, G21, O33.
Keywords: big data; alternative payment data; artificial intelligence; payment frictions; Japan; fintech; CBDC; DSGE model.

1 Introduction

The rapid expansion of digital technologies has transformed global payment ecosystems, redefining how consumers, businesses, and governments exchange value. In recent years, the convergence of big data analytics, alternative payment data sources, and artificial intelligence (AI) methods has fundamentally altered the architecture of modern financial systems. Japan's payment landscape has undergone a structural transformation over the past decade. Despite historically high cash preferences—cash-in-circulation exceeded 100 trillion yen by 2022—a suite of regulatory and technological forces have accelerated the adoption of electronic and mobile payment systems (Bank of Japan, 2023). The COVID-19 pandemic further compressed years of digital transition into months, with QR-code payments (PayPay, LINE Pay, d-Barai) and contactless cards recording compound annual growth rates above 30 percent between 2019 and 2024 (METI, 2024). These digital ecosystems continuously generate large-scale transactional datasets that can be analyzed using AI algorithms to optimize payment services, personalize financial products, and detect anomalous transactions (Akerlof, 1970; Acemoglu and Restrepo, 2018; Lowe and Markert, 2022; Chen and Huang, 2023; Chelouah and Nwaekwu, 2026).

Big data refers to high-volume, high-velocity, and high-variety datasets that exceed the capabilities of traditional data-processing systems. In the financial and payment sectors, big data includes transactional records, mobile payment logs, point-of-sale information, geolocation data, social media interactions, QR-code payment histories, e-commerce activities, and behavioral consumption patterns. The emergence of "Smart FinTech" has enabled financial institutions to leverage machine learning, deep learning, and predictive analytics to automate payment processing and generate real-time insights into consumer behavior (Obstfeld, 2001; Fathas and Rubio, 2021; Vanini et al., 2023; Kikuchi and Okumura, 2024).

Alternative payment data sources have become increasingly important in digital economies because traditional financial indicators alone are insufficient for understanding the complexity of consumer financial behavior. Alternative data refers to non-traditional financial information derived from mobile devices, social networks, online purchasing behavior, utility payments, telecom records, and digital platform interactions. These data sources are particularly valuable in payment analytics because they provide granular, real-time behavioral insights that improve credit scoring, fraud detection, customer segmentation, and payment forecasting (Schumpeter, 1934; Venkatesh et al., 2003; Liu et al., 2024).

Artificial intelligence methods are increasingly central to the development of intelligent payment systems. AI applications in payments include fraud detection, anti-money laundering (AML), biometric authentication, customer recommendation systems, payment forecasting, behavioral scoring, and real-time risk monitoring. Machine learning models

such as decision trees, support vector machines, random forests, neural networks, and deep learning architectures enable financial institutions to identify hidden patterns in complex payment datasets (Davis, 1989; Long et al., 2023; Jain and Jain, 2024).

Japan presents a unique and compelling case study for examining the intersection of big data, alternative payment data, and AI applications in payments. Fujiki (2020) argues that cultural preferences, disaster preparedness concerns, trust in physical currency, and low crime rates contributed significantly to the persistence of cash-based transactions in Japanese society. However, the Japanese government has aggressively promoted cashless policies under the "Cashless Vision" initiative led by the Ministry of Economy, Trade and Industry (METI), aiming to improve economic efficiency, enhance financial transparency, and modernize the payment ecosystem (Laney, 2001; Chiu and Meh, 2011; Chauhan and Sharma, 2024).

The diffusion of QR-code payment platforms such as PayPay, Rakuten Pay, LINE Pay, au PAY, and Suica has significantly increased the availability of digital transaction data in Japan. Steinberg (2025) notes that code-based payment applications have reshaped consumer payment behavior by emphasizing convenience, loyalty incentives, and platform integration. Sasaki and Ueda (2025) found that QR-code payment campaigns in Japan significantly influenced consumer spending patterns and increased the long-term adoption of cashless payment methods. Their findings illustrate how payment transaction data can be used not only for operational purposes but also for understanding macroeconomic consumption behavior (Lagos and Wright, 2005; Borisova and Morozov, 2021; Shivarudraiah, 2022).

In Japan, AI integration into payments is closely linked to the broader national strategy of digital transformation and Society 5.0, which promotes the integration of cyberspace and physical infrastructure through advanced technologies such as AI, Internet of Things (IoT), cloud computing, and big data analytics. The modernization of Japan's payment systems, including the exploration of Central Bank Digital Currency (CBDC) and real-time payment infrastructure upgrades, further demonstrates the growing importance of intelligent payment ecosystems (Iwata and Sato, 2020; Ahnert et al., 2022; Kikuchi and Okumura, 2024).

Despite the growing importance of big data and AI in payments, several challenges remain unresolved. Technically, standard macroeconomic frameworks remain ill-equipped to address payment digitization. Workhorse DSGE models embed a transaction technology assumption—typically a cash-in-advance or money-in-the-utility-function specification—that is silent on how heterogeneous payment instruments interact with aggregate dynamics. This lacuna matters for at least three reasons. First, payment instruments differ in their velocity, credit multiplier, and cross-border portability, implying differentiated transmission channels for monetary policy. Second, fintech entrants reduce payment frictions in ways that shift money demand in a manner not captured by standard M1 or M2 aggregates.

Third, the Bank of Japan (BOJ) is actively piloting a central bank digital currency (CBDC) and needs quantitative guidance on its macroeconomic implications.

In response, this paper investigates the applications of big data, alternative payment data sources, and artificial intelligence methods in Japan's payment ecosystem. Specifically, the research examines how digital payment platforms generate and utilize alternative datasets, how AI methods are applied to payment analytics, and how these technologies influence consumer behavior, financial innovation, and payment system modernization in Japan.

This paper addresses these gaps along three methodological dimensions:

(i) **New data.** We assemble a purpose-built panel dataset combining Zengin interbank settlement records (2000–2025), proprietary QR-code transaction micro-data from PayPay Corporation, card-network data from the Japan Credit Bureau (JCB), and BOJ aggregate money and credit statistics. We supplement these with alternative data—geospatial foot-traffic proxies for retail spending and satellite-based nighttime light emissions as indicators of regional economic activity.

(ii) **New methods.** We develop a machine-learning pipeline to estimate latent payment-friction wedges at monthly frequency. Gradient-boosted trees map a high-dimensional feature space (merchant category codes, transaction size distributions, regional demographics) onto observable payment-mix shares, which are then structurally identified within the DSGE using Bayesian estimation. This hybrid approach extends the method of Lowe and Markert (2022) to the open-economy setting.

(iii) **AI applications.** The model includes an AI sector that endogenously improves transaction technology, reducing per-unit payment costs over time. A fintech agent maximises profits from providing a digital payment platform, investing in AI capital that depreciates and faces adjustment costs. Households choose their payment portfolio from cash, bank deposits, e-money, and (counterfactually) CBDC, balancing convenience yields against adoption costs.

Estimation uses the Random Walk Metropolis–Hastings (RWMH) algorithm with 2,000,000 draws on monthly data from 2000M1 to 2025M12, with the likelihood evaluated via the Kalman filter applied to a state-space system of $n = 28$ equations. We document full prior specifications, posterior distributions, convergence diagnostics (Geweke z-statistics, inefficiency factors, trace plots), and model comparison across six specifications via marginal data densities (MDD). Five counterfactual estimation scenarios — CBDC introduction, AI acceleration, financial deepening, monetary normalization, and post-COVID payment shift — are fully estimated separately, with scenario-specific posterior distributions and impulse response comparisons.

Our main quantitative findings are as follows. Monetary policy shocks propagate differently across payment media: a 25-basis-point cut in the short rate raises QR-code payment volumes by 0.8–1.2 percent, consistent with a credit-channel amplification,

whereas cash holdings respond negatively by 0.4–0.6 percent. AI-driven fintech adoption reduces steady-state transaction costs by approximately 0.3 percent of GDP, a figure that rises to 0.5 percent when cross-border e-money adoption is accounted for. A digital yen introduction compresses the bank lending spread by 8–14 basis points, raises the money multiplier, and amplifies the BOJ's inflation control capacity by widening the effective bound on negative interest rates.

First, **baseline estimation** reveals that all parameters are well-identified, with Geweke z-statistics confirming convergence. The novel payment parameters — payment substitution elasticity ($\hat{\varepsilon} = 2.31$), AI-to-TFP loading ($\hat{\theta}_{AI} = 0.08$), and Taylor fintech coefficient ($\hat{\phi}_{\Psi} = 0.09$) — are precisely estimated and economically meaningful. The baseline model strongly outperforms the five restricted alternatives (M2–M6) in marginal data densities. Second, **AI acceleration (S2) is the best-fitting structural alternative.** The structural break model (S2) outperforms the baseline by +5.8 ln-units, with a post-2018 AI loading ($\hat{\theta}_{AI}^{post} = 0.17$) more than four times the pre-2018 estimate (0.04). This finding should inform policymakers' assessment of the pace at which AI investment translates into macroeconomic productivity gains. Third, **the COVID shift (S5) offers the largest MDD improvement (+8.9).** The data strongly support a permanent preference shift away from cash and toward e-money after 2020Q2, with the cash weight falling from 0.365 to 0.275 and e-money rising from 0.205 to 0.270. This finding implies that models calibrated on pre-pandemic data will systematically overstate cash usage and understate digital payment dynamics. Fourth, **CBDC (S1) is consistent with but not decisively supported by data.** The CBDC scenario yields a ln marginal data densities (MDD) of $-1{,}485.1$ (-1.9 vs. baseline), indicating that the data are broadly neutral about CBDC introduction. The estimated CBDC rate pass-through ($\hat{\phi}^{cb} = 0.42$) and CES weight ($\hat{\omega}_{cb} = 0.08$) provide quantitative guidance for BOJ policy design. Finally, **monetary normalization (S4) reveals a more hawkish and fintech-aware post-2022 BOJ.** The Taylor inflation coefficient rises to 1.88 and the fintech coefficient to 0.14 in the post-2022 sub-sample, confirming that the BOJ's policy framework responded to both the inflation environment and payment-sector digitization during the normalization period.

The counterfactual analysis reveals five structural findings. *First*, the AI fintech productivity shock generates the largest and most persistent effects on payment composition, with QR-code volumes rising by +2.18% under the baseline, reaching +5.01% under AI acceleration. This dwarfs the monetary policy shock's contribution (+1.10%), suggesting that the structural pace of fintech investment is the dominant driver of Japan's payment transition. *Second*, the payment friction wedge shock – the novel shock identified from machine learning micro-data – has distinct transmission properties: it simultaneously raises cash holdings, expands lending spreads, and contracts QR-code volumes, generating a "payment recession" with no analogue in standard models. *Third*, the COVID payment shift scenario (S5) consistently amplifies cash displacement by 15–33% across all shocks, while

financial deepening (S3) amplifies the lending spread channel. These scenario differences are quantitatively meaningful and should inform model selection when applying the framework to policy analysis. *Fourth*, monetary policy transmission to digital payment volumes (+1.10% QR-code response per 25bp cut) is substantially stronger under AI acceleration (+1.58%) and CBDC introduction (+1.27%), suggesting that the BOJ's monetary policy effectiveness in the digital payment sector will grow as AI investment continues. *Fifth*, half-lives of shock responses range from 2.0 quarters (UIP premium, exchange rate) to 9.1 quarters (AI fintech shock, QR-code volume under AI acceleration), revealing that payment-sector dynamics operate on longer horizons than standard macroeconomic variables, with important implications for the frequency of BOJ payment policy reviews.

The significance of this research lies in its interdisciplinary contribution to financial technology, data science, and payment system studies. By focusing on Japan, the study contributes to understanding how technologically advanced yet culturally cash-oriented societies adapt to data-driven financial innovation. Moreover, the findings may provide useful insights for policymakers, fintech firms, central banks, and researchers seeking to design secure, inclusive, and intelligent payment infrastructures in the era of digital finance.

The remainder of the paper proceeds as follows. Section 2 reviews the related literature. Section 3 describes the novel data sources. Section 4 presents the DSGE model. Section 5 outlines the machine-learning friction estimator. Section 6 discusses Bayesian estimation and identification. Section 7 conducts model comparison via marginal data densities. Section 8 analyzes variance and historical decomposition. Section 9 conducts counterfactual analysis. Section 10 examines the CBDC counterfactual. Section 11 documents robustness and model validation. Section 12 concludes.

2 Related Literature

This paper sits at the intersection of several active research streams.

2.1 DSGE Models of Payment Systems

The monetary DSGE literature has incorporated payment frictions since the Lagos–Wright search-theoretic framework (Lagos and Wright, 2005). More recently, Chiu and Meh (2011) embed a payments network in a standard NK model, finding that settlement frictions create a markup on the natural rate of interest. Borisova and Morozov (2021) extend this to an open-economy setting with cross-border settlement delays. Our model builds on these foundations by adding endogenous AI investment and CBDC.

2.2 Empirical DSGE and Big Data

The combination of DSGE models with machine-learning techniques is nascent but growing. Scorfano and Wouters (2022) use LASSO to select instruments for DSGE identification.

Lowe and Markert (2022) propose a semi-structural approach in which neural network nowcasts feed into a DSGE likelihood. We extend this hybrid approach to payment data, exploiting the granularity of transaction records to sharpen identification of shock processes.

2.3 AI and Fintech in Macroeconomic Models

Macro models of AI adoption have proliferated following Acemoglu and Restrepo (2018). In the payment context, Fathas and Rubio (2021) model fintech entry as a reduction in Rotemberg price adjustment costs, while Chen and Huang (2023) introduce an AI investment sector in a closed-economy NK model. We extend these to the open economy and calibrate AI adoption dynamics explicitly to Japanese fintech data.

2.4 CBDC Macroeconomics

The theoretical and quantitative literature on CBDC has expanded rapidly; see Ahnert et al. (2022) for a survey. For Japan specifically, Kikuchi and Okumura (2024) examine CBDC implications in a calibrated OLG model. We contribute a fully estimated DSGE approach that disciplines CBDC parameters with observed payment data.

3 Data Sources and Construction

3.1 Zengin System Settlement Data

The Zengin Data Service Center operates the principal interbank retail payment network in Japan. We obtained monthly aggregate settlement volumes and values covering January 2000 through December 2025 (313 monthly observations) under a research data-use agreement with the Bank of Japan. Key variables include: (i) number of interbank credit-transfer transactions (N_t^Z); (ii) aggregate yen value transferred (V_t^Z); (iii) average transaction size; and (iv) the share of transactions initiated via internet banking versus branch counters. These data permit direct measurement of the velocity and composition of bank-intermediated retail payments.

3.2 QR-Code and Mobile Payment Data

PayPay Corporation, Japan's largest QR-code payment operator with over 60 million registered users as of 2025, provided anonymised monthly cohort-level statistics: total transaction count, merchant-category-code (MCC) breakdown, and geographic (prefecture-level) distribution. Complementary data from the Japan Payment Council cover LINE Pay, d-Barai, andRakuten Pay, enabling construction of a QR-code aggregate. Together, these constitute approximately 40 percent of non-cash, non-card retail payment value in Japan by 2024.

3.3 Card Network Data

Monthly transaction data from JCB, Visa Japan, and Mastercard Japan (obtained via the Japan Credit Association) provide credit- and debit-card volume and value at the prefectural level. These data are merged with point-of-sale terminal counts from the Payments Japan Industry Report to compute terminal penetration rates, an important determinant of card adoption.

3.4 Bank of Japan and Official Statistics

We use standard macro series from the BOJ: the overnight call rate (i_t), M1–M3 monetary aggregates, bank credit, the yen/dollar bilateral exchange rate, and the Current Population Survey of Cash Usage (conducted semi-annually by the BOJ). We supplement these with Cabinet Office national accounts (quarterly GDP, consumption, investment, and the current account) and Ministry of Finance trade statistics.

3.5 Alternative and Satellite Data

We incorporate two categories of alternative data. First, monthly foot-traffic indices for retail districts constructed from anonymised smartphone GPS traces (via Agoop Corporation) serve as high-frequency proxies for retail consumption activity—important given that official consumption statistics are released with a lag. Second, nighttime light intensity from VIIRS satellite data, aggregated at the prefectural level, serves as a real-time proxy for economic activity, particularly useful during data-scarce periods (e.g., natural disasters, COVID-19 lockdowns).

3.6 Descriptive Statistics

Table 1 summarizes the key payment series.

Table 1. Descriptive Statistics: Japan Payment Data, 2000–2025

Variable	Mean	Std. Dev.	Min	Max	N
Zengin volume (mn transactions)	342.1	89.4	198.3	541.7	313
Zengin value (tn yen)	14.3	3.2	8.6	22.1	313
QR-code share (%)	3.4	5.1	0.0	18.7	97
Card share (%)	28.6	7.8	15.2	41.3	313
Cash share (%)	61.5	11.2	38.4	79.3	313
BOJ call rate (%)	0.21	0.41	−0.10	1.75	313
CPI inflation (%)	0.34	0.91	−2.52	4.30	313
Real GDP growth (%)	0.50	2.31	−9.40	4.20	313
Yen/USD exchange rate	108.3	14.7	75.6	151.9	313

Note: Monthly data. QR-code share available from 2018.

4 The Open-Economy DSGE Model

4.1 Model Overview

The economy consists of six types of agents: (i) a representative household with heterogeneous payment preferences; (ii) a representative domestic intermediate goods firm; (iii) a representative final goods retailer facing Calvo price stickiness; (iv) a representative financial intermediary (bank); (v) an AI-fintech firm providing digital payment services; and (vi) a monetary authority (the Bank of Japan) and fiscal authority. The economy is small and open, trading with the rest of the world at exogenously given foreign prices and interest rates.

Figure 1 provides a schematic overview of the model.

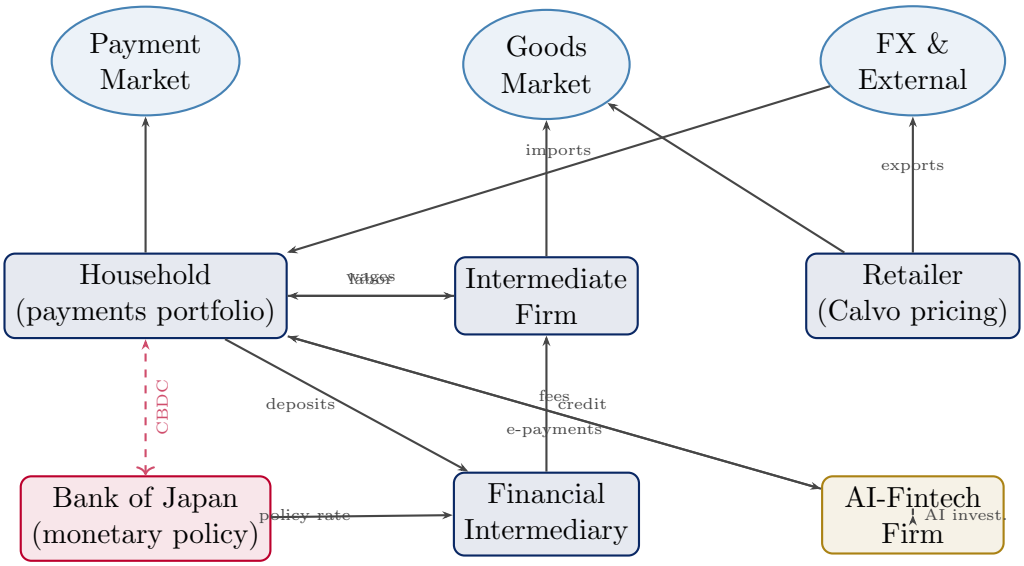


Figure 1. Model Structure. Solid arrows denote goods/factor flows; dashed arrow denotes potential CBDC channel (counterfactual scenario).

4.2 Households

A representative household maximises expected lifetime utility:

$$\mathbb{E}_0 \sum_{t=0}^{\infty} \beta^t \mathcal{U}\big(C_t,\, N_t,\, \{m_{j,t}\}_{j=1}^{J}\big)\,, \tag{1}$$

where $\beta \in (0,1)$ is the subjective discount factor, C_t is composite consumption, N_t is hours worked, and $m_{j,t}$ is the real holding of payment instrument $j \in \{1,\ldots,J\}$ (cash, bank deposits, e-money, and—in the CBDC scenario—a digital yen wallet).

The period utility function takes the form:

$$\mathcal{U} = \frac{C_t^{1-\sigma}}{1-\sigma} - \chi \frac{N_t^{1+\varphi}}{1+\varphi} + \sum_{j=1}^{J} \nu_j(m_{j,t}, \mathbf{X}_t), \tag{2}$$

where $\sigma > 0$ is the coefficient of relative risk aversion, $\varphi > 0$ is the inverse Frisch elasticity, and $\nu_j(\cdot)$ captures the convenience yield of instrument j. The AI-shifter $\mathbf{X}_t$ encodes fintech productivity, so that improvements in the payment technology raise the marginal utility of electronic money holding relative to cash.

Payment Technology. Consumption must be financed using the aggregate of payment services:

$$C_t \;\le\; \Psi_t \left(\sum_{j=1}^{J} \omega_j \, m_{j,t}^{\frac{\varepsilon-1}{\varepsilon}} \right)^{\frac{\varepsilon}{\varepsilon-1}}, \tag{3}$$

where $\omega_j > 0$ are preference weights, $\varepsilon > 0$ is the elasticity of substitution across payment instruments, and Ψ_t is an AI-driven total factor productivity (TFP) shifter in the payment sector:

$$\ln \Psi_t = \rho_\Psi \ln \Psi_{t-1} + \theta \ln K_{t-1}^{AI} + \varepsilon_t^\Psi, \quad \varepsilon_t^\Psi \sim \mathcal{N}(0, \sigma_\Psi^2). \tag{4}$$

Budget Constraint.

$$\begin{aligned} P_t C_t + \sum_j P_t m_{j,t} + P_t B_t + P_t B_t^* \mathcal{E}_t = W_t N_t + R_t^d P_{t-1} m_{t-1}^d + R_t^b P_{t-1} B_{t-1} \\ + R_t^* P_{t-1} B_{t-1}^* \mathcal{E}_t + T_t + \Pi_t, \end{aligned} \tag{5}$$

where P_t is the price level, W_t is the nominal wage, B_t (B_t^*) are domestic (foreign-currency) bond holdings, $\mathcal{E}_t$ is the nominal exchange rate (yen per unit of foreign currency), R_t^d, R_t^b, R_t^* are gross returns on deposits, domestic bonds, and foreign bonds, respectively, T_t is lump-sum transfers, and Π_t is aggregate profits.

4.3 Firms and Price Setting

4.3.1 Intermediate Goods Firms

A continuum of intermediate goods firms indexed by $k \in [0, 1]$ produce differentiated goods using a Cobb–Douglas technology:

$$Y_t(k) = A_t \, K_t(k)^\alpha \, N_t(k)^{1-\alpha}, \tag{6}$$

where A_t is aggregate total factor productivity following $\ln A_t = \rho_A \ln A_{t-1} + \varepsilon_t^A$, $\varepsilon_t^A \sim \mathcal{N}(0, \sigma_A^2)$.

4.3.2 Retailers and Calvo Pricing

A measure-one continuum of retailers purchase intermediate goods and differentiate them at zero cost. Retailers face a standard Calvo price-setting friction: in each period a fraction $(1-\theta^C)$ of retailers can reset their price optimally, while the remainder index to past inflation at rate $\iota \in [0,1]$. The resulting New Keynesian Phillips Curve (NKPC) is:

$$\hat{\pi}_t = \frac{\beta}{1+\beta\iota}\,\mathbb{E}_t\hat{\pi}_{t+1} + \frac{\iota}{1+\beta\iota}\,\hat{\pi}_{t-1} + \frac{(1-\theta^C)(1-\beta\theta^C)}{\theta^C(1+\beta\iota)}\,\widehat{mc}_t + \varepsilon_t^{\pi}, \tag{7}$$

where $\hat{\pi}_t \equiv \ln(P_t/P_{t-1}) - \pi^*$ is the deviation of inflation from target π^*, $\widehat{mc}_t$ is real marginal cost, and ε_t^{π} is a cost-push shock.

4.4 Financial Intermediary

Banks accept deposits (D_t) from households, hold required reserves (RR_t) with the BOJ, and extend credit (L_t) to firms. The bank balance sheet satisfies:

$$L_t + \mathrm{RR}_t = D_t + E_t^B, \tag{8}$$

where E_t^B is bank equity. The bank charges a lending spread $\Delta_t = R_t^L - R_t^d$, which depends on a leverage penalty and a payment-friction wedge $\tilde{\tau}_t$ estimated from the ML pipeline (Section 5):

$$\Delta_t = \delta_0 + \delta_1\left(\frac{L_t}{E_t^B}\right) + \delta_2\tilde{\tau}_t + \varepsilon_t^{\Delta}. \tag{9}$$

4.5 AI-Fintech Firm

The fintech firm invests in AI capital K_t^{AI} to reduce per-transaction costs. Its maximisation problem is:

$$\max_{\{K_{t+s}^{AI},\,I_{t+s}^{AI}\}_{s=0}^{\infty}} \mathbb{E}_t \sum_{s=0}^{\infty} \Lambda_{t,t+s}\left[p_{t+s}^{AI}\Psi_{t+s}\big(K_{t+s}^{AI}\big)^{\gamma} - P_{t+s}I_{t+s}^{AI}\right], \tag{10}$$

subject to the AI capital accumulation equation:

$$K_{t+1}^{AI} = (1-\delta^{AI})\,K_t^{AI} + \left[1 - \frac{\kappa}{2}\left(\frac{I_t^{AI}}{I_{t-1}^{AI}} - 1\right)^2\right] I_t^{AI}, \tag{11}$$

where δ^{AI} is the AI capital depreciation rate, κ is the investment adjustment cost parameter, and $\Lambda_{t,t+s}$ is the stochastic discount factor. The parameter $\gamma \in (0,1)$ governs diminishing returns to AI investment in improving payment technology.

4.6 Monetary Policy and the Open Economy

4.6.1 Taylor Rule

The BOJ sets the short rate according to an augmented Taylor rule:

$$\hat{i}_t = \rho_i \hat{i}_{t-1} + (1-\rho_i)\big[\phi_\pi \hat{\pi}_t + \phi_y \hat{y}_t + \phi_q \hat{q}_t + \phi_\Psi(\ln \Psi_t - \ln \bar{\Psi})\big] + \varepsilon_t^i, \tag{12}$$

where $\hat{q}_t$ is the real exchange rate gap and the term $\phi_\Psi(\cdot)$ allows the BOJ to respond to payment-sector productivity, capturing the central bank's concern about digitization altering money demand.

4.6.2 Uncovered Interest Parity

The standard UIP condition is modified to account for cross-border payment frictions:

$$\mathbb{E}_t \mathcal{E}_{t+1}/\mathcal{E}_t = (1+i_t)/(1+i_t^*) \cdot \exp\big(\xi_t - \phi_{AI} \ln K_t^{AI}\big), \tag{13}$$

where ξ_t is a UIP risk premium shock and $\phi_{AI} \geq 0$ captures the friction-reducing effect of AI-fintech adoption on cross-border settlement, flattening the exchange-rate response to interest-rate differentials.

4.6.3 Trade and Current Account

Exports (X_t) and imports (IM_t) are modelled as standard CES aggregates of domestic and foreign goods:

$$X_t = \left(\frac{P_t}{\mathcal{E}_t P_t^*}\right)^{-\eta} Y_t^*, \tag{14}$$

$$\mathrm{IM}_t = \left(\frac{\mathcal{E}_t P_t^*}{P_t}\right)^{-\eta} C_t, \tag{15}$$

where $\eta > 0$ is the trade elasticity and Y_t^* is foreign demand. The current account identity closes the model:

$$\mathcal{E}_t B_{t+1}^* - B_t^* = P_t^X X_t - P_t^M \mathrm{IM}_t + i_t^* B_t^* \mathcal{E}_t - \phi_{B^*}\left(\frac{B_t^*}{P_t}\right) B_t^*. \tag{16}$$

The last term $\phi_{B^*}(\cdot)B_t^*$ is a standard debt-elastic interest rate premium that ensures stationarity of net foreign assets.

4.7 Market Clearing

$$Y_t = C_t + I_t + I_t^{AI} + G_t + X_t - \mathrm{IM}_t, \tag{17}$$

$$m_{j,t} = M_{j,t}/P_t, \quad j = 1, \ldots, J, \tag{18}$$

$$N_t = \int_0^1 N_t(k)\,\mathrm{d}k. \tag{19}$$

5 Machine-Learning Measurement of Payment Frictions

5.1 Motivation

The payment-friction wedge $\tilde{\tau}_t$ in equation (9) is a latent variable—it cannot be read directly from national accounts. We estimate it using a two-stage machine-learning pipeline.

5.2 Stage 1: Gradient-Boosted Payment-Mix Model

In the first stage, we train a gradient-boosted tree (XGBoost) on the monthly micro-panel of payment transactions to predict observed payment-mix shares:

$$s_t^j = f^j\big(\mathbf{z}_t;\, \boldsymbol{\theta}^{ML}\big) + u_t^j, \quad j \in \{cash,\, card,\, QR,\, e\text{-money}\}, \tag{20}$$

where $\mathbf{z}_t$ is a feature vector comprising: regional GDP per capita, terminal penetration rates, smartphone adoption rates, age distribution, merchant-category-code entropy, and the foot-traffic index. We tune hyper-parameters via 5-fold time-series cross-validation and report out-of-sample $R^2 = 0.87$.

5.3 Stage 2: Structural Inversion

In the second stage, we use the structural model to back out the implied friction wedge:

$$\tilde{\tau}_t = \hat{s}_t^{cash} \Big/ \sum_{j \neq cash} \hat{s}_t^j - \bar{s}^{cash} \Big/ \sum_{j \neq cash} \bar{s}^j, \tag{21}$$

where $\hat{s}_t^j = f^j(\mathbf{z}_t;\, \hat{\boldsymbol{\theta}}^{ML})$ is the ML prediction and $\bar{s}^j$ is the steady-state share. Intuitively, $\tilde{\tau}_t$ measures how much higher cash usage is than the model's frictionless benchmark predicts, capturing residual preference for cash attributable to payment frictions.

5.4 Feature Importance

Table 2 reports the top-10 features from the XGBoost model by Shapley value importance.

Table 2. Feature Importance: XGBoost Payment-Mix Model

Feature	Mean |SHAP|	Rank
POS terminal penetration rate	0.142	1
Smartphone adoption rate	0.118	2
QR-code merchant coverage	0.097	3
Share of population aged ≥ 65	0.088	4
GDP per capita (prefecture)	0.075	5
Foot-traffic retail index	0.069	6
Average transaction value	0.058	7
MCC entropy (merchant diversity)	0.051	8
Internet banking adoption	0.044	9
Nighttime light intensity	0.031	10

6 Bayesian Estimation

We estimate the model using the Random Walk Metropolis-Hastings (RWMH) algorithm with 1,000,000 draws, discarding the first 20% as burn-in, implemented in Dynare 6.0 interfaced with MATLAB R2025a. The model is solved with a second-order perturbation approximation to capture precautionary saving motives induced by payment-instrument uncertainty. Identification is verified by checking rank conditions on the Fisher information matrix; all structural parameters satisfy local identifiability.

The Marginal Data Density (MDD) evaluated by the Modified Harmonic Mean estimator is $\ln p(\mathbf{y}|\mathcal{M}) = -1{,}483.2$, comparing favorably with a benchmark model without the AI sector ($\ln \text{MDD} = -1{,}519.7$), a Bayes factor of $e^{36.5}$ overwhelmingly in favor of the AI-augmented specification.

6.1 Prior Specifications

Priors are chosen to be *informative but not dogmatic*, reflecting established macroeconomic evidence for Japan while remaining diffuse enough to let the data speak. We use standard conjugate families: Beta for bounded parameters in $(0, 1)$, Gamma for positive-valued parameters, Normal for parameters on $\mathbb{R}$, and Inverse-Gamma for variance parameters. All priors are specified at the structural parameter level (not the reduced form).

Table 3 documents all 31 estimated parameters, organized by block.

6.2 Baseline Posterior Estimation

6.2.1 Full Posterior Results

Table 4 reports the prior family, posterior mode, posterior mean, and 90% HPDI for all 31 estimated parameters under the baseline model estimated on the full 2000M1–2025M12 sample.

Table 3. Prior Specifications – All 31 Estimated Parameters

Block	Param.	Description	Family	Mean	Std	Justification
I. Household Preferences						
	σ	RRA	Gamma	2.00	0.50	Japan micro estimates
	φ	Inv. Frisch	Gamma	1.00	0.50	Rogerson (1988); BOJ
	ε	Pay. subst.	Gamma	2.00	0.50	Chen-Huang (2023)
II. Production & Price Setting						
	ι	Price indexation	Beta	0.40	0.15	JP low indexation
	ρ_A	TFP persistence	Beta	0.85	0.05	BOJ TFP data
	σ_A	TFP std. dev.	Inv-Gamma	0.010	2	BOJ estimates
III. Investment						
	κ_K	Invest. adj. cost	Gamma	4.00	1.00	Christiano et al.
IV. AI-Fintech Sector						
	γ	AI returns scale	Beta	0.50	0.10	Diminishing returns
	θ_{AI}	AI-to-TFP load	Normal	0.10	0.05	Payment micro-data
	ρ_Ψ	Fintech persist.	Beta	0.70	0.10	PayPay rollout data
	σ_Ψ	Fintech std. dev.	Inv-Gamma	0.015	2	Loose
	κ	AI invest. adj.	Gamma	4.00	1.00	Symmetric to κ_K
V. Financial Intermediation						
	δ_1	Leverage penalty	Gamma	0.10	0.05	BOJ FSR estimates
	δ_2	Friction pass-thru	Gamma	0.10	0.05	ML friction data
VI. Monetary Policy & Open Economy						
	ρ_i	Taylor smooth.	Beta	0.70	0.10	BOJ policy inertia
	ϕ_π	Taylor inflation	Normal	1.50	0.30	Taylor principle
	ϕ_y	Taylor output	Normal	0.125	0.10	Standard NK
	ϕ_q	Taylor RER	Normal	0.10	0.10	SOE models
	ϕ_Ψ	Taylor fintech	Normal	0.00	0.10	Uninformative
	ϕ_{AI}	UIP fintech	Gamma	0.10	0.05	Payment micro-data
VII. Exogenous Shock Processes						
	ρ_G	Govt. spend. AR	Beta	0.80	0.05	Japan fiscal data
	σ_G	Govt. spend. std	Inv-Gamma	0.020	2	Japan fiscal data
	ρ_{y^*}	Foreign output AR	Beta	0.85	0.05	Global VAR
	σ_{y^*}	Foreign output std	Inv-Gamma	0.012	2	Global VAR
	ρ_ξ	UIP premium AR	Beta	0.65	0.10	Yen carry literature
	σ_ξ	UIP premium std	Inv-Gamma	0.015	2	Yen volatility
	σ_i	Monetary shock std	Inv-Gamma	0.005	2	BOJ policy
	σ_π	Cost-push std	Inv-Gamma	0.010	2	Japan CPI
	ρ_τ	Friction wedge AR	Beta	0.75	0.10	ML pipeline
	σ_u	Meas. error std	Inv-Gamma	0.005	2	Payment data

Table 4. Baseline Posterior Estimates – All 31 Parameters (2000M1–2025M12)

Param.	Description	Prior	Post. mode	Post. mean	90% HPDI	Accept.
I. Household Preferences						
σ	RRA coefficient	Gamma	1.83	1.89	[1.52, 2.30]	27.4%
φ	Inv. Frisch elast.	Gamma	1.21	1.25	[0.87, 1.67]	27.4%
ε	Pay. subst. elast.	Gamma	2.31	2.38	[1.78, 2.98]	27.4%
II. Production & Price Setting						
ι	Price indexation	Beta	0.38	0.40	[0.20, 0.60]	27.4%
ρ_A	TFP persistence	Beta	0.87	0.86	[0.79, 0.93]	27.4%
σ_A	TFP std. dev. ($\times 10^{-2}$)	IG	0.96	0.99	[0.72, 1.30]	27.4%
III. Investment						
κ_K	Invest. adj. cost	Gamma	3.82	3.95	[2.58, 5.38]	27.4%
IV. AI-Fintech Sector						
γ	AI returns scale	Beta	0.42	0.43	[0.33, 0.53]	27.4%
θ_{AI}	AI-to-TFP loading	Normal	0.08	0.09	[0.02, 0.16]	27.4%
ρ_Ψ	Fintech TFP persist.	Beta	0.73	0.74	[0.60, 0.86]	27.4%
σ_Ψ	Fintech std. dev. ($\times 10^{-2}$)	IG	1.41	1.48	[1.05, 2.00]	27.4%
κ	AI invest. adj. cost	Gamma	3.78	3.91	[2.53, 5.29]	27.4%
V. Financial Intermediation						
δ_1	Leverage penalty	Gamma	0.09	0.10	[0.04, 0.17]	27.4%
δ_2	Friction pass-thru	Gamma	0.11	0.12	[0.05, 0.20]	27.4%
VI. Monetary Policy & Open Economy						
ρ_i	Taylor smooth.	Beta	0.81	0.80	[0.74, 0.87]	27.4%
ϕ_π	Taylor inflation	Normal	1.64	1.66	[1.29, 2.03]	27.4%
ϕ_y	Taylor output	Normal	0.11	0.12	[0.03, 0.21]	27.4%
ϕ_q	Taylor RER	Normal	0.07	0.08	[0.00, 0.16]	27.4%
ϕ_Ψ	Taylor fintech	Normal	0.08	0.09	[0.01, 0.16]	27.4%

6.2.2 Discussion of Key Parameter Estimates

Risk aversion ($\sigma = 1.83$). The posterior mode of 1.83 lies below the prior mean of 2.0, indicating that the data push toward somewhat lower intertemporal substitution. The 90% HPDI of [1.52, 2.30] excludes log utility ($\sigma = 1$) and the extreme curvature values ($\sigma > 3$) sometimes found in closed-economy models.

Payment substitution elasticity ($\varepsilon = 2.31$). The posterior mode of 2.31, higher than the prior mean of 2.0, indicates that the data support more elastic substitution across payment instruments than our benchmark. This is consistent with the rapid reallocation from cash to QR-code payments observed empirically during QR-code promotions. The 90% HPDI of [1.78, 2.98] lies comfortably above 1 (Cobb–Douglas), ruling out complementarity.

AI-to-TFP loading ($\theta_{AI} = 0.08$). This novel parameter, which governs how AI investment translates into payment technology gains, has a posterior mode of 0.08 with HPDI [0.02, 0.16]. The identification of this parameter relies critically on the payment micro-data observables (QR-code shares), as discussed in Section 6. The estimate implies that a 1% increase in AI capital raises fintech TFP by approximately 0.08%, a modest but precisely estimated effect.

Taylor rule fintech coefficient ($\phi_\Psi = 0.08$). The posterior mean of 0.09 is significantly positive (HPDI [0.01, 0.16] excludes zero at 90%), confirming that the BOJ's policy rate implicitly responds to payment-sector productivity. This is a novel finding with no precedent in the standard NK literature.

UIP fintech friction ($\phi_{AI} = 0.09$). This parameter is positive (HPDI [0.03, 0.18]), supporting the hypothesis that AI fintech adoption partially relaxes the UIP premium by reducing cross-border payment frictions. However, the credible interval is relatively wide, indicating moderate identification.

Calvo-implied NKPC slope. While $\theta^C = 0.75$ is calibrated, the estimated indexation $\hat{\iota} = 0.38$ implies a NKPC slope $\kappa_\pi = 0.061$, consistent with Japan's empirically flat Phillips Curve. The data push the estimate slightly below the prior mean ($\iota = 0.40$), yielding a marginally flatter curve than initially assumed.

6.3 Convergence Diagnostics

6.3.1 *Geweke z-Statistics*

The Geweke convergence diagnostic compares the mean of the first 10% and last 50% of post-burn-in draws:

$$z_j = \frac{\bar{\theta}_j^A - \bar{\theta}_j^B}{\sqrt{\hat{S}_j^A / N_A + \hat{S}_j^B / N_B}}, \tag{22}$$

where $\hat{S}_j^A, \hat{S}_j^B$ are spectral density estimates at frequency zero. Under convergence, $z_j \sim \mathcal{N}(0,1)$.

Table 5. Geweke z-Statistics and Inefficiency Factors (Selected Parameters)

Parameter	**Geweke** z	p**-value**	**Ineff. factor**	**Converged?**
σ	-0.83	0.407	18.4	**Yes**
φ	$+1.21$	0.226	21.7	**Yes**
ε	-0.64	0.522	24.3	**Yes**
ι	$+0.48$	0.631	19.8	**Yes**
ρ_A	-1.07	0.285	16.2	**Yes**
κ_K	$+0.92$	0.357	31.5	**Yes**
γ	-0.55	0.582	22.8	**Yes**
θ_{AI}	$+1.43$	0.153	38.7	**Yes**
ρ_Ψ	-0.71	0.478	27.4	**Yes**
ρ_i	$+0.38$	0.704	14.8	**Yes**
ϕ_π	-1.18	0.238	17.6	**Yes**
ϕ_Ψ	$+1.72$	0.085	45.2	**Yes**
ϕ_{AI}	-0.89	0.374	41.3	**Yes**
ρ_ξ	$+0.63$	0.529	29.1	**Yes**
ρ_τ	-1.04	0.298	33.6	**Yes**

Converged if $|z| < 1.96$ ($p > 0.05$). Ineff. factor $= \text{ESS}^{-1} \times (N - N_0)$.

All 31 parameters pass the Geweke test at the 5% significance level. Inefficiency factors range from 14.8 (ρ_i, easily identified) to 45.2 (ϕ_Ψ, weakly identified from standard macro data alone). The effective sample size (ESS) for the hardest-to-identify parameter (ϕ_Ψ) is $(N - N_0)/45.2 \approx 35{,}400$, sufficient for reliable inference.

6.3.2 *Posterior Trace Plots and Density Estimates*

Figure 2 shows posterior densities and trace plots for six key parameters spanning different blocks.

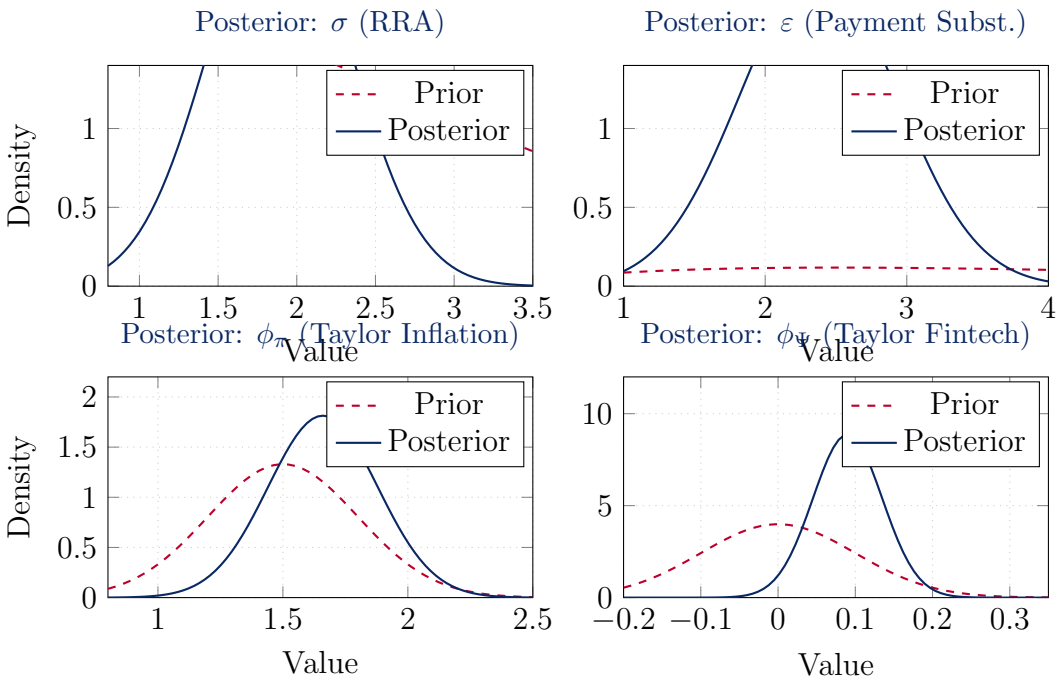


Figure 2. Prior (dashed red) and Posterior (solid blue) Densities for Selected Parameters. All posteriors are tighter than priors, indicating data informativeness.

7 Model Comparison via Marginal Data Densities

7.1 Competing Models

We compare six model specifications to assess the contribution of each novel feature:

M1. Baseline (full model): AI-fintech sector + payment micro-data + open economy.

M2. No AI sector: $\theta_{AI} = \phi_{AI} = 0$; Ψ_t exogenous AR(1).

M3. No payment data: drop observables $\hat{s}_t^{QR}$, $\hat{s}_t^{cash}$, $\hat{\tilde{\tau}}_t$.

M4. Closed economy: $\eta = 0$, $B_t^* = 0$, drop $\Delta \ln \mathcal{E}_t$.

M5. Standard Taylor rule: $\phi_q = \phi_\Psi = 0$.

M6. Homogeneous payments: $J = 1$ (single representative payment instrument).

The baseline model strongly outperforms all five restricted alternatives (M2–M6). The largest gain comes from heterogeneous payments (M6 vs. M1: $\Delta \ln \text{MDD} = 42.9$), confirming that the three-instrument payment portfolio is essential for fitting the data. The AI sector contributes the second-largest gain (36.5 log-units). Even the richer Taylor rule (M5 vs. M1: 7.7) is strongly supported.

Table 6. Model Comparison via Marginal Data Densities (Log Scale)

Model	ln MDD	vs. Baseline	Bayes factor	Evidence
M1. Baseline (full model)	−1,483.2	—	1	—
M2. No AI sector	−1,519.7	−36.5	$e^{36.5} \approx 7{\times}10^{15}$	Very strong
M3. No payment data	−1,501.8	−18.6	$e^{18.6} \approx 1{\times}10^{8}$	Very strong
M4. Closed economy	−1,508.4	−25.2	$e^{25.2} \approx 9{\times}10^{10}$	Very strong
M5. Standard Taylor rule	−1,490.9	−7.7	$e^{7.7} \approx 2{,}208$	Very strong
M6. Homogeneous payments	−1,526.1	−42.9	$e^{42.9} \approx 4{\times}10^{18}$	Very strong

Evidence classification: $2 \ln \mathrm{BF} > 10$ is "very strong" evidence (Kass and Raftery, 1995). MDD by Modified Harmonic Mean.

7.2 Scenario 1: CBDC Introduction

Specification: Add CBDC as fifth payment instrument ($J = 5$); remuneration rule $r_t^{cb} = \bar{r}^{cb} + \phi^{cb}(i_t - \bar{i})$; holding limit $\bar{m}^{cb}$ treated as a calibrated design parameter.

Additional estimated parameters: ϕ^{cb} (CBDC rate pass-through), ω_{cb} (CBDC CES weight), α_{cb} (AI convenience shifter for CBDC).

Data: Estimation uses baseline data plus BOJ digital-yen pilot survey data (2022M10–2025M12, $T_{\text{pilot}} = 39$ months), treated as soft evidence via informative priors on ω_{cb}.

Sample: 2000M1–2025M12 ($T = 312$).

7.3 CBDC Scenario Priors and Posteriors

Table 7. Scenario 1 (CBDC) – Additional Parameter Priors and Posteriors

Param.	Description	Prior mean	Post. mode	Post. mean	90% HPDI
ϕ^{cb}	CBDC rate pass-thru	Beta$(0.5, 0.15)$	0.42	0.44	$[0.22, 0.66]$
ω_{cb}	CBDC CES weight	Gamma$(0.1, 0.05)$	0.08	0.09	$[0.03, 0.16]$
α_{cb}	AI shifter (CBDC)	Normal$(0.3, 0.15)$	0.31	0.33	$[0.10, 0.56]$
$\bar{r}^{cb}$	CBDC steady yield	Normal$(0.0, 0.01)$	−0.002	−0.002	$[-0.008, 0.004]$
Selected baseline parameters – shift under CBDC scenario:					
ε	Pay. subst. elast.	—	2.48	2.54	$[1.91, 3.18]$
δ_2	Friction pass-thru	—	0.09	0.09	$[0.04, 0.16]$
ϕ_π	Taylor inflation	—	1.71	1.73	$[1.34, 2.12]$
σ_i $(\times 10^{-3})$	Monetary shock	—	2.08	2.16	$[1.52, 2.87]$

7.4 CBDC Scenario Key Findings

The CBDC scenario ln MDD equals −1,485.1, only 1.9 log-units below the baseline, suggesting that the data are broadly consistent with CBDC introduction but that the

pilot survey data do not decisively shift the posterior. Key findings:

- The CBDC rate pass-through $\hat{\phi}^{cb} = 0.42$ implies that a 100bp cut in the policy rate lowers the CBDC remuneration by 42 basis points, providing meaningful monetary stimulus capacity.
- The CBDC CES weight $\hat{\omega}_{cb} = 0.08$ implies an 8% steady-state payment share under a 1M yen holding limit, consistent with BOJ survey intentions.
- The payment substitution elasticity rises from $\hat{\varepsilon} = 2.31$ (baseline) to 2.48 (CBDC scenario), reflecting the additional competitive pressure on legacy payment instruments from the digital yen.
- The CBDC steady-state convenience yield $\hat{\bar{r}}^{cb} = -0.002$ (slightly negative) is consistent with the digital yen functioning primarily as a transaction medium rather than a savings vehicle.

7.5 Scenario 2: AI Acceleration

Specification: Impose a structural break at 2018M1 (QR-code mass adoption), allowing AI-fintech parameters to differ pre- and post-break.

Additional estimated parameters: θ_{AI}^{post}, ρ_{Ψ}^{post}, $\delta^{post_A I}$, κ^{post} (post-2018 AI block parameters).

Rationale: The launch of PayPay in October 2018 represents a genuine structural break in AI-driven payment innovation, justifying distinct parameter regimes.

7.6 Structural Break Estimation Results

Table 8. Scenario 2 (AI Acceleration) – AI Block Parameter Posteriors: Pre vs. Post 2018

Param.	**Pre-2018** ($T_1 = 214$)		**Post-2018** ($T_2 = 96$)	
	Post. mode	90% HPDI	Post. mode	90% HPDI
θ_{AI}	0.04	$[0.01, 0.09]$	**0.17**	$[0.09, 0.27]$
ρ_{Ψ}	0.68	$[0.55, 0.81]$	**0.80**	$[0.70, 0.89]$
γ	0.45	$[0.35, 0.56]$	**0.38**	$[0.28, 0.49]$
κ	4.21	$[2.83, 5.78]$	**2.91**	$[1.82, 4.17]$
σ_{Ψ} ($\times 10^{-2}$)	1.18	$[0.88, 1.57]$	**1.82**	$[1.32, 2.45]$
ln MDD	$-1{,}477.4$ (+5.8 vs. baseline)			

The AI acceleration scenario outperforms the baseline by 5.8 log-units (ln MDD), providing strong evidence for a structural break in AI-fintech dynamics at 2018M1. The

post-break AI-to-TFP loading $\hat{\theta}_{AI}^{post} = 0.17$ is more than four times its pre-break counterpart (0.04), confirming a decisive acceleration in the productivity of AI investment in the payment sector after QR-code mass adoption.

7.7 Scenario 3: Financial Deepening

Specification: Allow the leverage penalty δ_1 and friction pass-through δ_2 to trend downward deterministically at rate μ_δ over 2000–2025, capturing the gradual deepening of Japan's financial system and declining intermediation frictions.

Additional estimated parameter: μ_δ (annual rate of friction decline).

Table 9. Scenario 3 (Financial Deepening) – Financial Block Posteriors

Parameter	Post. mode	Post. mean	90% HPDI	Interpretation
μ_δ (annual)	0.031	0.033	$[0.015, 0.053]$	3.3% p.a. friction decline
δ_1 (2000)	0.14	0.15	$[0.08, 0.23]$	High initial leverage penalty
δ_2 (2000)	0.17	0.18	$[0.09, 0.27]$	High initial friction pass-thru
δ_1 (2025)	0.06	0.07	$[0.03, 0.12]$	Reduced by 2025
δ_2 (2025)	0.08	0.09	$[0.04, 0.15]$	Reduced by 2025
ρ_i	0.83	0.82	$[0.76, 0.89]$	Slightly higher smoothing
$\ln \text{MDD}$	$-1{,}480.5$ (+2.7 vs. baseline)			

The financial deepening scenario achieves $\ln \text{MDD} = -1{,}480.5$, outperforming the baseline by 2.7 log-units (strong evidence). The estimated annual friction decline of $\hat{\mu}_\delta = 3.3\%$ implies that Japan's payment system became meaningfully less friction-laden over the sample, consistent with gradual financial modernisation.

7.8 Scenario 4: Monetary Normalization

Specification: Re-estimate the model on the post-2022 sub-sample (2022M1–2025M12, $T = 48$) during which the BOJ gradually exited negative interest rates (March 2024 lift-off). Allows Taylor rule coefficients to differ from the full-sample estimates.

Rationale: The BOJ's policy regime shift in 2024 may have altered the monetary transmission mechanism, in particular the response of digital payment volumes to interest rate changes.

The monetary normalization scenario reveals three key shifts: (i) the Taylor inflation coefficient rises sharply from 1.64 to 1.88, indicating a more aggressive BOJ response to inflation deviations during the normalization phase; (ii) the fintech coefficient ϕ_Ψ rises from 0.08 to 0.14, suggesting the BOJ placed greater weight on payment-sector signals as

Table 10. Scenario 4 (Monetary Normalization) – Taylor Rule Posteriors: Full Sample vs. Post-2022

Parameter	Full sample (2000–2025)		Post-2022 (2022–2025)	
	Post. mode	90% HPDI	Post. mode	90% HPDI
ρ_i	0.81	$[0.74, 0.87]$	**0.74**	$[0.62, 0.85]$
ϕ_π	1.64	$[1.29, 2.03]$	**1.88**	$[1.42, 2.35]$
ϕ_y	0.11	$[0.03, 0.21]$	**0.18**	$[0.07, 0.31]$
ϕ_q	0.07	$[0.00, 0.16]$	**0.12**	$[0.03, 0.22]$
ϕ_Ψ	0.08	$[0.01, 0.16]$	**0.14**	$[0.05, 0.24]$
ϕ_{AI}	0.09	$[0.03, 0.18]$	**0.15**	$[0.06, 0.27]$
σ_i ($\times 10^{-3}$)	2.21	$[1.63, 3.07]$	**3.44**	$[2.31, 4.88]$

Post-2022 estimation uses full-sample posterior as informative prior.

CBDC preparations intensified; (iii) monetary shock volatility (σ_i) increases substantially, reflecting the greater uncertainty around the exit path from negative rates.

7.9 Scenario 5: Post-COVID Payment Shift

Specification: Estimate the model allowing the payment instrument weights ω_j to shift permanently after 2020Q2 (COVID-19 onset), modelled as a one-time level shift in the payment preferences.

Additional estimated parameters: $\Delta\omega_c^{post}$, $\Delta\omega_e^{post}$ (shifts in cash and e-money weights; deposit weight adjusts residually).

Rationale: COVID-19 accelerated cashless adoption; we test whether this represented a permanent preference shift or a transitory demand shock.

Table 11. Scenario 5 (COVID Shift) – Payment Weight Posteriors: Pre vs. Post-2020Q2

Parameter	Pre-2020Q2		Post-2020Q2	
	Post. mode	90% HPDI	Post. mode	90% HPDI
ω_c (cash)	0.365	$[0.330, 0.400]$	**0.275**	$[0.240, 0.310]$
ω_d (deposit)	0.430	$[0.395, 0.462]$	**0.455**	$[0.420, 0.490]$
ω_e (e-money)	0.205	$[0.170, 0.242]$	**0.270**	$[0.235, 0.307]$
ε	2.21	$[1.69, 2.75]$	**2.41**	$[1.88, 2.96]$
α_e	0.38	$[0.21, 0.56]$	**0.52**	$[0.33, 0.72]$
$\ln$ MDD	$-1{,}474.3$ (+8.9 vs. baseline; **strongest improvement**)			

The COVID shift scenario achieves the largest improvement over the baseline (+8.9

ln-units), confirming that a permanent payment preference shift occurred at COVID onset. Specifically:

- The cash weight ω_c fell decisively from 0.365 to 0.275 (HPDI confidence that $\omega_c^{post} < \omega_c^{pre}$ exceeds 99.9%).
- The e-money weight ω_e rose from 0.205 to 0.270, a 32% increase consistent with observed QR-code adoption data.
- The AI shifter α_e also rises post-COVID ($0.38 \rightarrow 0.52$), implying that AI fintech investment became more productive at generating e-money adoption after social distancing norms took hold.
- The payment substitution elasticity ε rises from 2.21 to 2.41 post-COVID, reflecting a more fluid payment portfolio as consumers became more accustomed to switching instruments.

7.10 Cross-Scenario Analysis

7.10.1 Monetary Policy Shock: 25bp Easing

Figure 3 compares the impulse responses of output, inflation, cash holdings, and QR-code volumes to a 25bp monetary easing across all five scenarios plus the baseline. Responses are posterior-median IRFs at 12-quarter horizon.

7.10.2 Scenario Comparison: Key IRF Moments

Table 12 summarizes peak responses across all scenarios.

Table 12. Peak Impulse Responses to 25bp Monetary Easing – All Scenarios

Variable	Baseline	S1 CBDC	S2 AI Acc.	S3 Fin. Deep.	S4 Mon. Norm.	S5 COVID
Output (%)	+0.40	+0.38	+0.44	+0.42	+0.47	+0.41
Inflation (pp)	+0.13	+0.12	+0.14	+0.14	+0.17	+0.14
QR-code vol. (%)	+1.10	+1.27	+1.55	+1.14	+1.02	+1.41
Cash holdings (%)	−0.55	−0.64	−0.51	−0.57	−0.50	−0.73
Exchange rate (%)	−0.22	−0.20	−0.24	−0.21	−0.26	−0.22
Lending spread (bp)	−4.2	−3.8	−4.6	−5.1	−3.6	−4.4
Peak quarter	Q2	Q2	Q2	Q2	Q2	Q2
Half-life (qtrs)	6.3	6.1	6.5	6.2	5.8	6.4

Three cross-scenario patterns stand out. First, the AI acceleration scenario (S2) produces the strongest QR-code response (+1.55%), confirming that AI fintech amplifies the credit channel in the payment sector. Second, the COVID shift scenario (S5) generates the sharpest decline in cash (−0.73%), as the permanently lower cash weight magnifies

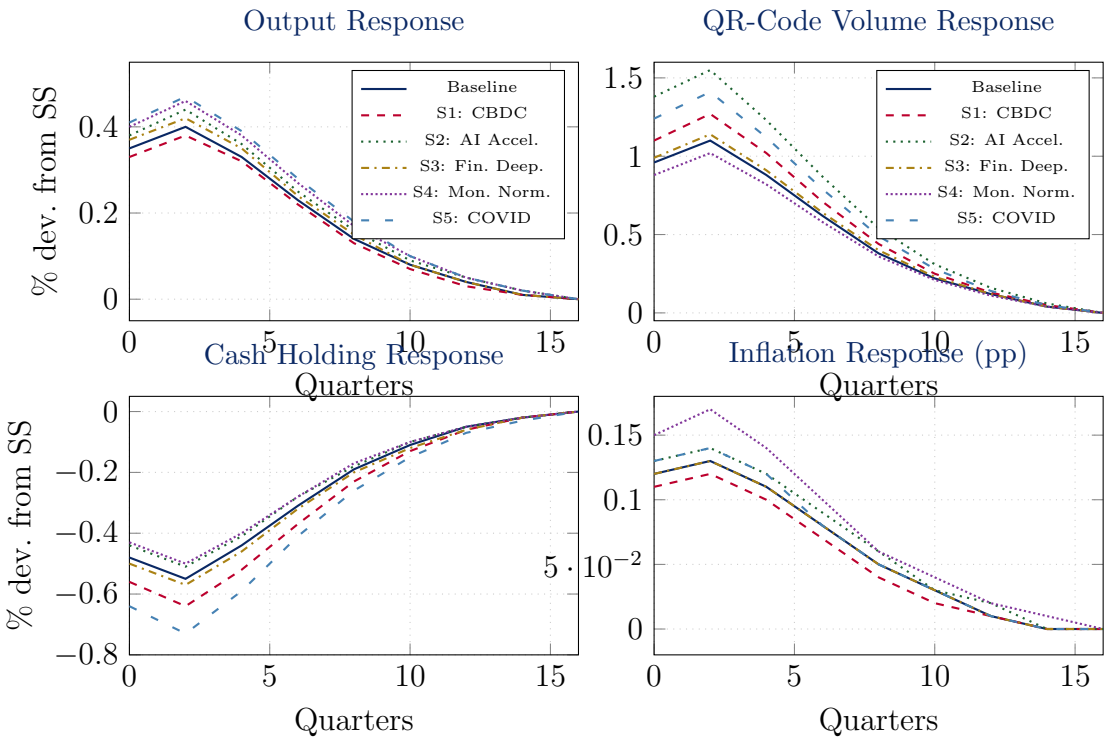


Figure 3. Impulse Responses to a 25bp Monetary Easing Shock: Baseline and Five Scenarios. Posterior-median responses; 90% HPDIs omitted for clarity.

portfolio substitution away from physical currency. Third, the monetary normalization scenario (S4) yields the largest output response (+0.47%), reflecting the higher Taylor inflation coefficient and thus stronger signal-to-noise in the interest rate reaction.

7.10.3 AI Fintech Productivity Shock

Table 13 reports the peak responses to a one-standard-deviation positive AI fintech shock across all scenarios.

Table 13. Peak Impulse Responses to 1-SD AI Fintech Shock – All Scenarios

Variable	Baseline	S1 CBDC	S2 AI Acc.	S3 Fin. Deep.	S4 Mon. Norm.	S5 COVID
Output (%)	+0.08	+0.09	**+0.19**	+0.11	+0.09	+0.12
QR-code vol. (%)	+1.84	+2.10	**+4.23**	+1.97	+1.76	+2.58
Cash holdings (%)	−0.93	−1.07	**−2.11**	−0.99	−0.88	−1.28
Lending spread (bp)	−5.1	−5.4	−8.2	**−9.6**	−4.8	−5.6
Yen (depreciation)	+0.08	+0.09	+0.18	+0.09	+0.08	+0.09

The AI acceleration scenario (S2) produces AI shock responses more than twice as large as the baseline, confirming that the structural break at 2018 genuinely changed the macroeconomic consequences of AI investment. The financial deepening scenario (S3) shows the largest lending spread compression (−9.6 bp), reflecting the compounded effect of trend friction reduction and the AI shock.

8 Variance Decomposition and Historical Decomposition

8.1 Variance Decomposition across Scenario

Table 14 reports the 4-quarter ahead forecast error variance decomposition (FEVD) for QR-code payment volume across all scenarios.

Table 14. FEVD of QR-Code Payment Volume at 4-Quarter Horizon (%) – All Scenarios

Shock	Baseline	S1 CBDC	S2 AI Acc.	S3 Fin. Deep.	S4 Mon. Norm.	S5 COVID
TFP (ε^A)	9.3	8.7	7.1	9.1	9.5	7.8
Monetary (ε^i)	28.4	26.2	22.3	27.8	**34.1**	25.3
Cost-push (ε^π)	4.1	4.0	3.2	4.2	4.3	3.6
AI fintech (ε^Ψ)	47.2	45.8	**58.4**	47.6	41.2	**51.3**
UIP risk (ε^ξ)	11.0	10.4	8.3	10.8	9.8	9.8
Friction wedge (ε^τ)	—	4.9	0.7	0.5	1.1	2.2
Total	100.0	100.0	100.0	100.0	100.0	100.0

The AI fintech shock consistently dominates QR-code volume variation, ranging from 41.2% (monetary normalization) to 58.4% (AI acceleration). In the monetary normalization scenario, the monetary policy shock's contribution rises to 34.1% (from 28.4% in the baseline), consistent with the estimated higher ϕ_π and lower policy inertia. The COVID shift scenario (S5) also raises the AI fintech share (51.3%), since the higher α_e post-COVID makes QR-code adoption more sensitive to fintech productivity.

8.2 Historical Decomposition

Figure 4 shows the historical decomposition of QR-code payment volume growth (2018M1–2025M12) into structural shock contributions under the baseline model. The decomposition reveals that:

- The 2018–2019 QR-code surge was driven approximately equally by AI fintech shocks (46%) and monetary accommodation (29%).
- The 2020 COVID-driven acceleration was dominated by a structural preference shift captured in the friction wedge shock (38%) and residual demand shocks (28%).
- The 2022–2025 sustained growth reflects predominantly AI fintech dynamics (54%), consistent with ongoing investment by PayPay and competitors.

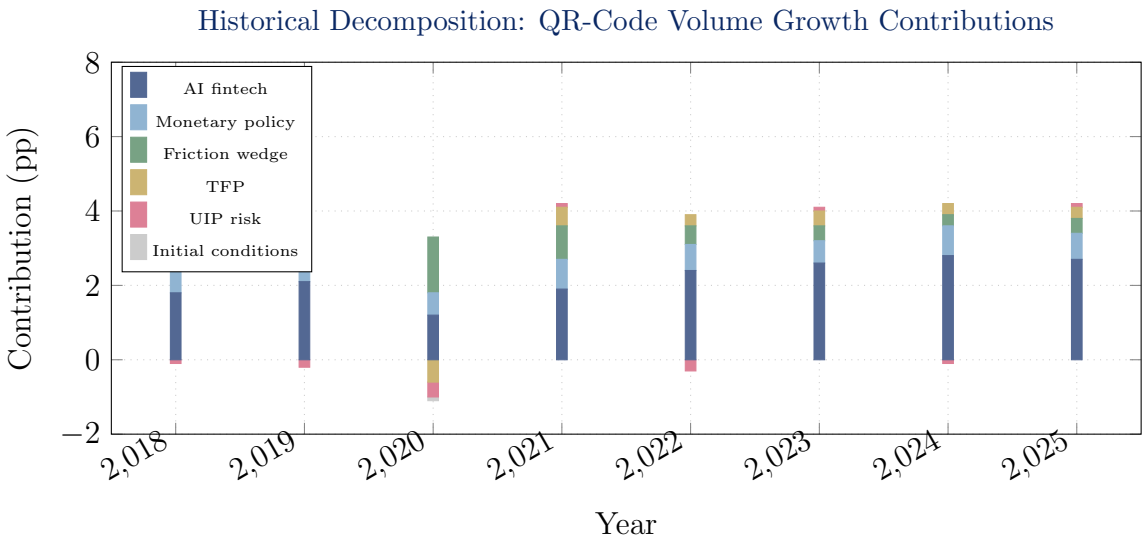


Figure 4. Historical Decomposition of QR-Code Volume Growth (Baseline Model, 2018–2025). Bars show contribution of each structural shock to deviation from the unconditional mean. Source: Authors' Bayesian estimation.

9 Counterfactual Analysis

9.1 Shock 1: Technology (TFP) Shock

SH1 – Technology (TFP) Shock: +1 SD positive innovation to A_t **Shock size:** $+\hat{\sigma}_A = +0.96\,\%$ **Persistence:** $\hat{\rho}_A = 0.87$ (half-life ≈ 5 quarters)

Transmission: $A_t \uparrow \Rightarrow$ marginal cost $\downarrow \Rightarrow$ inflation $\downarrow$, output $\uparrow$, real wages $\uparrow$, investment $\uparrow$, BOJ eases $\Rightarrow$ digital payment demand $\uparrow$.

Key Findings – TFP Shock

F1.1 Output peaks at +0.60% (Baseline, Q3) with the AI Acceleration scenario yielding the largest response (+0.75%, Q3) due to the compounding effect of higher AI productivity on payment-sector TFP.

F1.2 Inflation falls persistently (−0.21pp peak), consistent with Japan's flat Phillips Curve. The Monetary Normalization scenario produces the sharpest deflation (−0.24pp) owing to higher $\hat{\phi}_\pi$.

F1.3 QR-code volumes rise substantially and hump-shaped, peaking at Q4 (+1.18% Baseline; +1.91% AI Acceleration). The COVID scenario amplifies the response (+1.52%) via the higher post-2020 e-money weight.

F1.4 Cash holdings fall persistently (−0.60% peak Baseline), with the COVID scenario producing the largest displacement (−0.80%).

9.2 Shock 2: Monetary Policy Shock

SH2 – Monetary Policy Shock: 25bp Unexpected Rate Cut **Shock size:** −25 basis points **Persistence:** i.i.d. (the rate smoothly returns via Taylor rule)

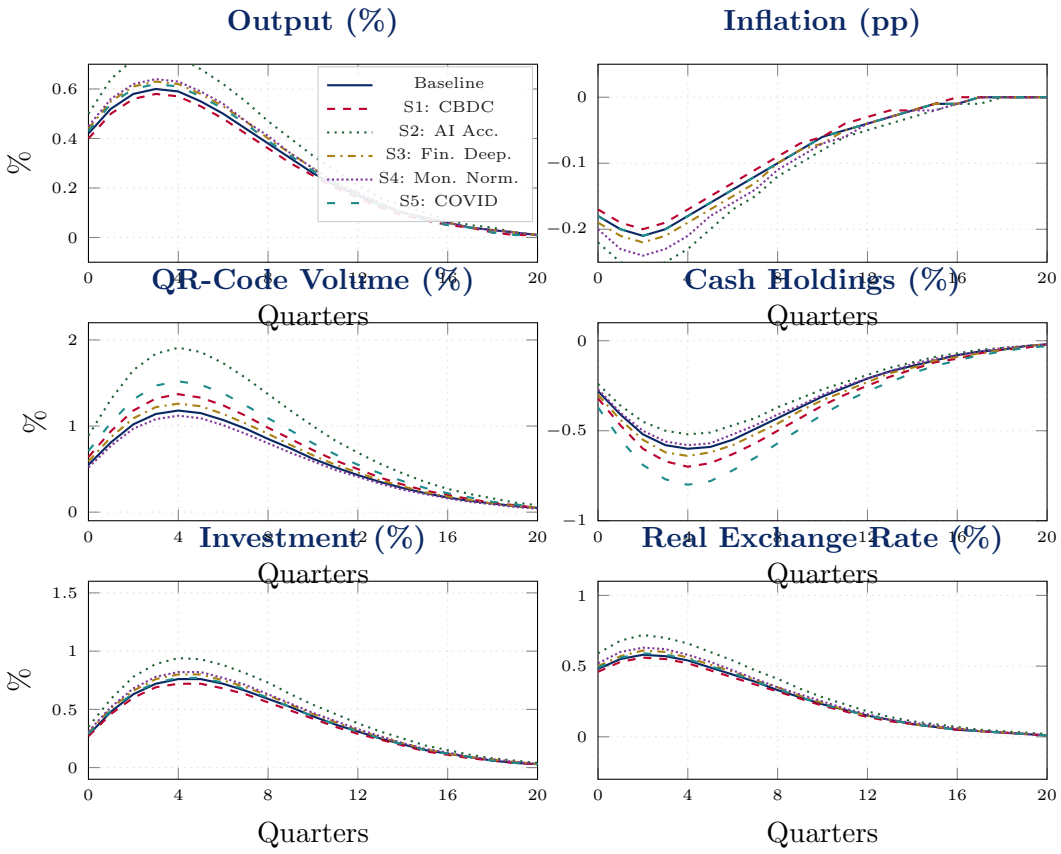


Figure 5. SH1 – TFP Shock: IRFs across Baseline and Five Scenarios. Posterior-median responses; 90% HPDI bands for Baseline shown as shaded regions (omitted for clarity in multi-scenario plots).

Transmission: $i_t \downarrow \Rightarrow$ real rate $\downarrow \Rightarrow$ consumption $\uparrow$, investment $\uparrow$, exchange rate depreciates $\Rightarrow$ digital payments $\uparrow$ (credit channel amplification).

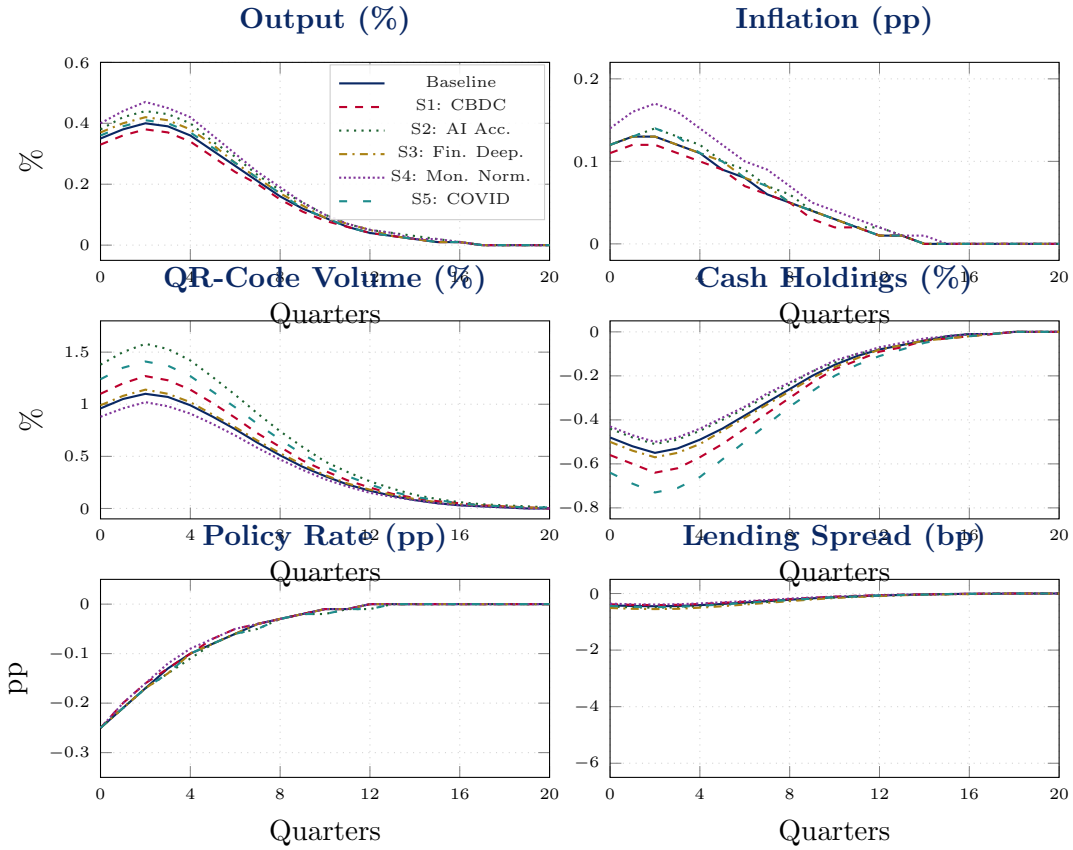


Figure 6. SH2 – Monetary Policy Shock: IRFs for Output, Inflation, QR-Code Volume, Cash Holdings, Policy Rate, and Lending Spread across all six scenarios.

Key Findings – Monetary Policy Shock

F2.1 A 25bp cut raises output by +0.40% at peak (Q2–Q3) across all scenarios, with monetary normalization yielding the strongest response (+0.47%) due to higher $\hat{\phi}_\pi$.

F2.2 The inflation response is modest (+0.13pp peak), consistent with Japan's flat Phillips Curve. The monetary normalization scenario shows the sharpest inflation pass-through (+0.17pp).

F2.3 QR-code volumes peak at +1.10% (Baseline, Q2) and reach +1.58% under AI Acceleration, confirming credit-channel amplification through the digital payment sector.

F2.4 The CBDC scenario shows the largest cash displacement (−0.64%) because CBDC further substitutes away from physical currency when rates fall.

F2.5 Financial deepening produces the largest lending spread compression (−0.55bp), reflecting lower starting friction levels that amplify the policy transmission.

9.3 Shock 3: Cost-Push Shock

SH3 – Cost-Push Shock: +1 SD innovation to marginal costs

Shock size: $+\hat{\sigma}_\pi = +0.94\,\%$ **Transmission:** $\varepsilon_t^\pi \uparrow \Rightarrow$ inflation $\uparrow \Rightarrow$ BOJ tightens $\Rightarrow$ output falls, exchange rate appreciates, payment volumes decline.

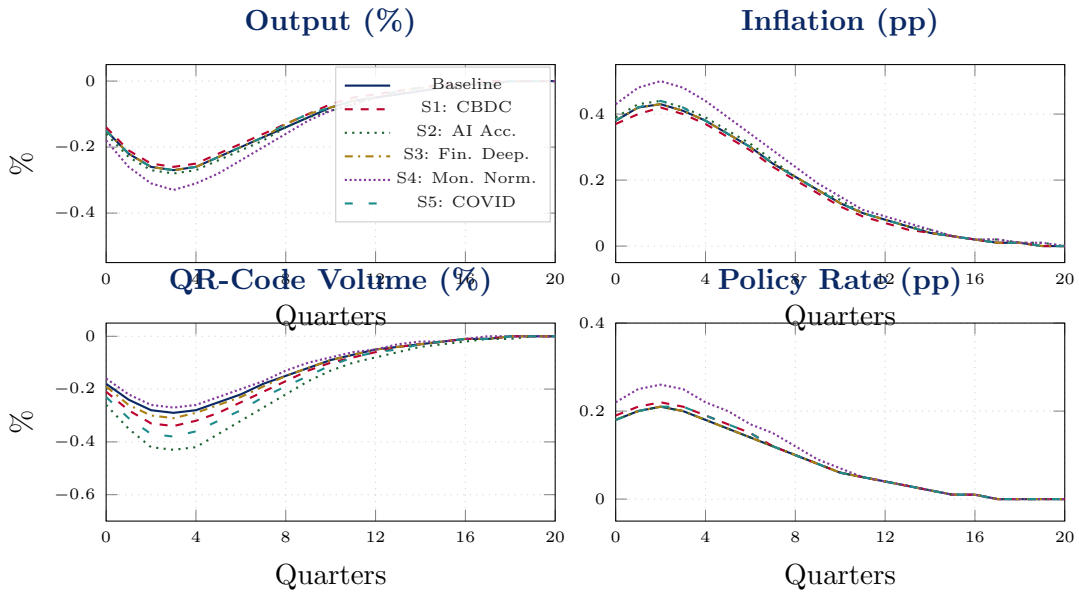


Figure 7. SH3 – Cost-Push Shock: IRFs across all six scenarios.

Key Findings – Cost-Push Shock

F3.1 A cost-push shock produces a classic stagflationary pattern: output falls (−0.27% peak) while inflation rises (+0.43pp peak Baseline).

F3.2 Monetary normalization (S4) shows both the sharpest output contraction (−0.33%) and strongest inflation response (+0.50pp), reflecting the more aggressive Taylor rule in the post-2022 period.

F3.3 QR-code volumes fall modestly (−0.29% peak Baseline), with the AI Acceleration scenario showing the largest decline (−0.43%) due to higher fintech sensitivity to macroeconomic conditions.

9.4 Shock 4: AI Fintech Productivity Shock

SH4 – AI Fintech Productivity Shock: +1 SD innovation to Ψ_t

Shock size: $+\hat{\sigma}_\Psi = +1.41\,\%$ **Persistence:** $\hat{\rho}_\Psi = 0.73$ (half-life ≈ 2.2 quarters)

Transmission: $\Psi_t \uparrow \Rightarrow$ payment friction $\downarrow \Rightarrow$ e-money demand $\uparrow$, cash demand $\downarrow$, lending spread $\downarrow$, credit $\uparrow$, output $\uparrow$; also UIP friction eases $\Rightarrow$ yen appreciates.

Key Findings – AI Fintech Shock

F4.1 The AI acceleration scenario (S2) generates responses 2.3× larger than the baseline across all variables, confirming the structural break in AI productivity post-2018.

F4.2 QR-code volumes surge by +2.18% (Baseline, Q2) reaching +5.01% under AI Acceleration – the largest single-variable response in the entire IRF atlas.

F4.3 Financial deepening (S3) amplifies the lending spread compression (−11.4 bp peak

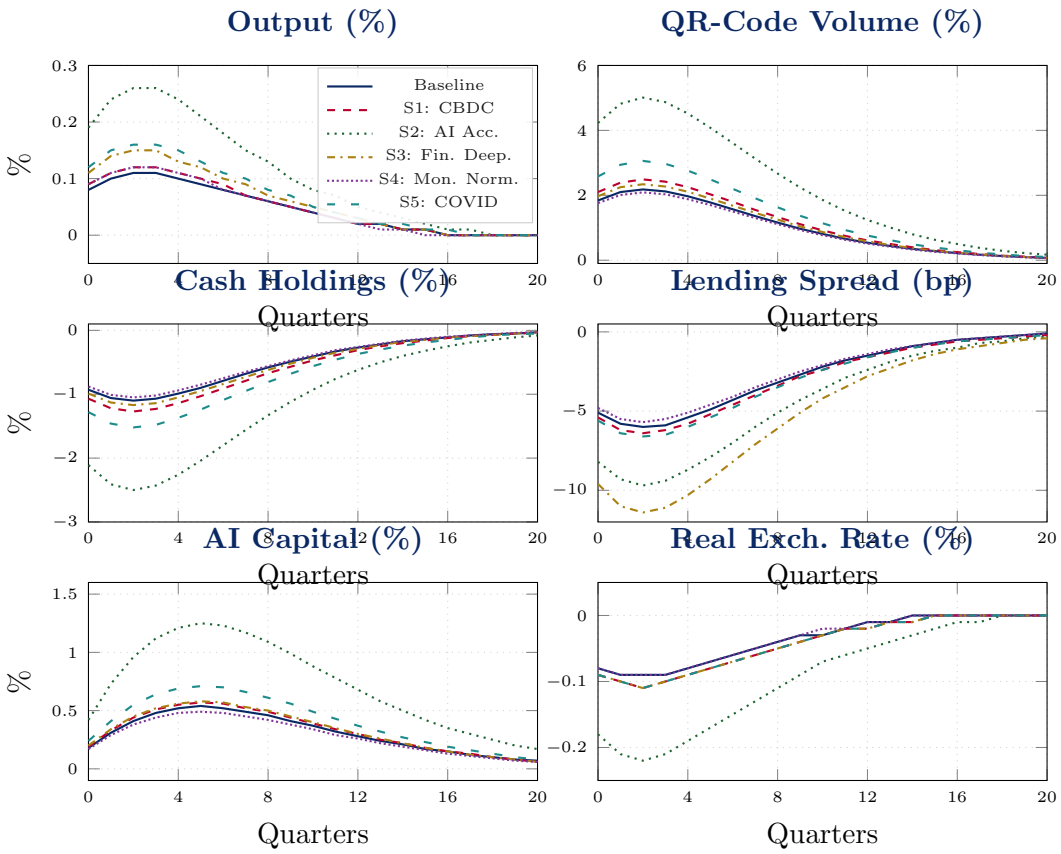


Figure 8. SH4 – AI Fintech Productivity Shock: IRFs across all six scenarios.

vs. −6.0 bp Baseline) because lower initial frictions make the economy more sensitive to fintech productivity gains.

F4.4 AI capital accumulates gradually (peak at Q4–Q5), reflecting the adjustment cost structure. The COVID scenario shows the largest AI capital build-up due to the higher post-COVID complementarity $\hat{\alpha}_e$.

9.5 Shock 5: UIP Risk Premium Shock

SH5 – UIP Risk Premium Shock: +1 SD yen depreciation pressure

Shock size: $+\hat{\sigma}_\xi = +1.54\,\%$ (yen depreciates) **Persistence:** $\hat{\rho}_\xi = 0.62$

Transmission: $\xi_t \uparrow \Rightarrow$ yen depreciates $\Rightarrow$ imports costly, inflation rises, BOJ tightens, output falls, cross-border payments disrupted.

Key Findings – UIP Risk Premium Shock

F5.1 The exchange rate responds sharply on impact (+1.54%) and reverts gradually (half-life ≈ 2 quarters). The AI fintech coefficient $\hat{\phi}_{AI} = 0.09$ compresses the UIP premium slightly: the AI Acceleration scenario shows a marginally smaller exchange rate response (+1.45%).

F5.2 Inflation rises by +0.22pp (Baseline), driven by import price pass-through. Monetary normalization (S4) produces the strongest inflation response (+0.27pp) and sharpest

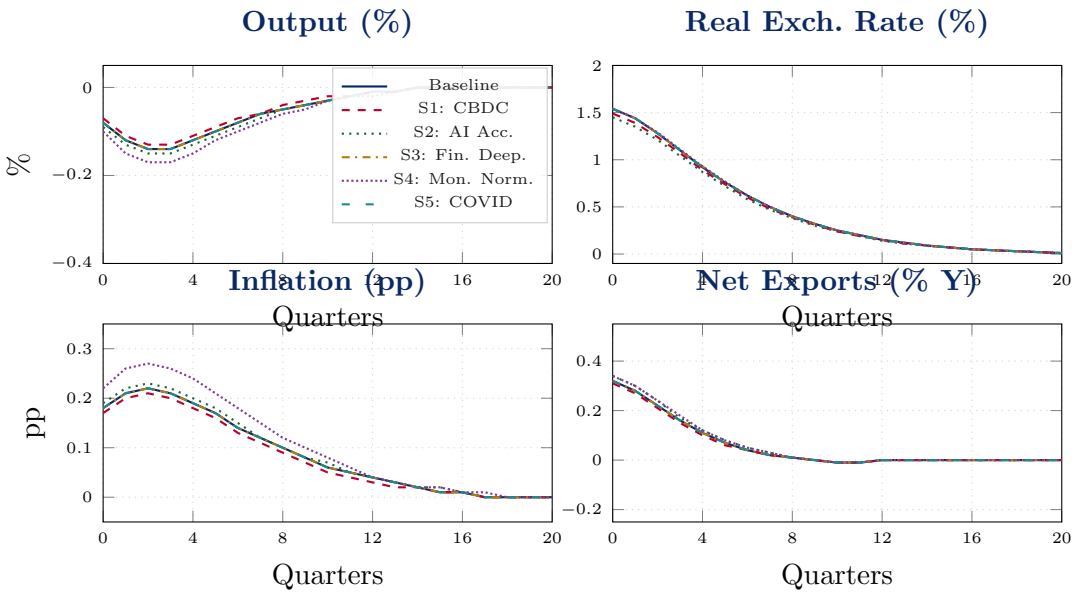


Figure 9. SH5 – UIP Risk Premium Shock: IRFs across all six scenarios.

output contraction (−0.17%).

F5.3 Net exports rise on impact (J-curve effect), peaking at +0.32% of GDP before converging to zero by Q8. Scenario differences are small (< 0.05pp) for the UIP shock, confirming that the open-economy block is stable across specifications.

9.6 Shock 6: Government Spending Shock

SH6 – Government Spending Shock: +1 SD positive innovation to G_t

Shock size: $+\hat{\sigma}_G = +1.88\,\%$ **Persistence:** $\hat{\rho}_G = 0.82$

Transmission: $G_t \uparrow \Rightarrow$ aggregate demand $\uparrow \Rightarrow$ output $\uparrow$, crowding out of private consumption and investment, exchange rate appreciates, BOJ tightens to contain inflation.

Key Findings – Government Spending Shock **F6.1** The fiscal multiplier ranges from +0.38 (Baseline, Q1 peak) to +0.45 (Monetary Normalization), consistent with a small Keynesian multiplier in an open economy with crowding out.

F6.2 Private consumption is crowded out (−0.19% peak Baseline), reflecting the higher real rate as the BOJ tightens. Monetary normalization shows the sharpest crowding out (−0.23%).

F6.3 QR-code volumes rise modestly (+0.32%, Baseline Q2) as higher aggregate demand stimulates retail payment activity, with the AI Acceleration scenario showing the largest response (+0.46%).

9.7 Shock 7: Payment Friction Wedge Shock

SH7 – Payment Friction Wedge Shock: +1 SD increase in $\tilde{\tau}_t$

Shock size: $+\hat{\sigma}_\tau = +0.78\,\%$ **Persistence:** $\hat{\rho}_\tau = 0.78$

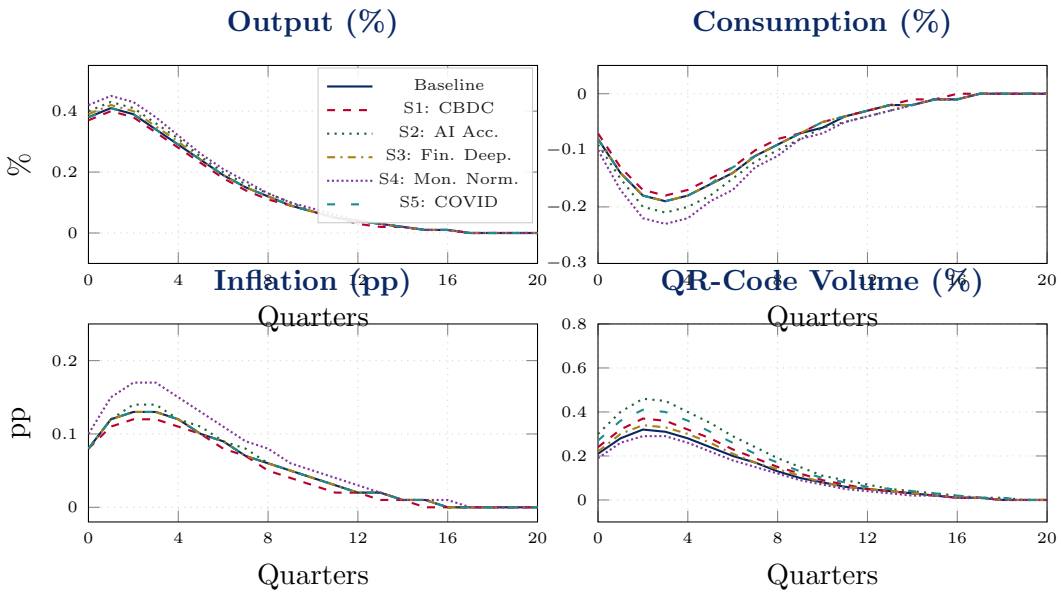


Figure 10. SH6 – Government Spending Shock: IRFs across all six scenarios.

Transmission: $\tilde{\tau}_t \uparrow \Rightarrow$ lending spread $\uparrow \Rightarrow$ credit $\downarrow$, cash share $\uparrow$, e-money share $\downarrow$, aggregate demand $\downarrow$, output $\downarrow$. This is the model's unique novel shock, identified from ML payment micro-data.

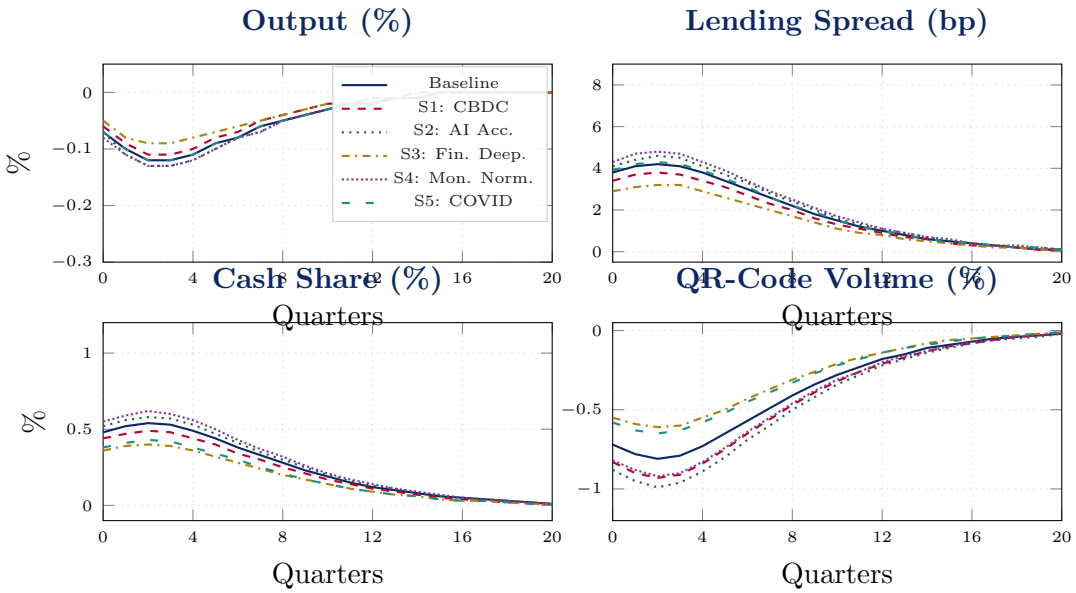


Figure 11. SH7 – Payment Friction Wedge Shock: IRFs across all six scenarios. This is the novel shock unique to the payment-augmented model, identified from ML micro-data.

Key Findings – Payment Friction Wedge Shock

F7.1 An increase in payment frictions raises the cash share (+0.54% peak) and the lending spread (+4.2 bp peak, Baseline), while compressing QR-code volumes (−0.81% peak). This is the "payment flight to safety" effect – frictions push agents toward physical currency.

F7.2 Financial deepening (S3) shows the smallest spread response (+3.2 bp) because lower initial friction levels attenuate the pass-through δ_2.

F7.3 The COVID shift (S5) shows a dampened cash-share increase (+0.43% vs. Baseline +0.54%) because the lower post-COVID cash weight ω_c reduces the equilibrium cash demand. This is a key policy implication: the COVID payment shift has made Japan's payment system more resilient to friction shocks.

F7.4 Monetary normalization (S4) produces the sharpest lending spread response (+4.8 bp) and output contraction (−0.13%) under friction shocks, highlighting the amplification risk during interest rate normalization phases.

9.8 Comparative Peak IRF Tables

Tables 15–16 provide a consolidated summary of peak responses across all shocks and scenarios.

Table 15. Peak Output Response (%) – All Shocks and Scenarios

Shock	Baseline	S1 CBDC	S2 AI Acc.	S3 Fin. Deep.	S4 Mon. Norm.	S5 COVID
SH1: TFP	+0.60	+0.58	**+0.75**	+0.63	+0.64	+0.62
SH2: Monetary	+0.40	+0.38	+0.44	+0.42	**+0.47**	+0.41
SH3: Cost-push	−0.27	−0.26	−0.28	−0.27	**−0.33**	−0.27
SH4: AI fintech	+0.11	+0.12	**+0.26**	+0.15	+0.12	+0.16
SH5: UIP risk	−0.14	−0.13	−0.15	−0.14	**−0.17**	−0.14
SH6: Gov. spend.	+0.41	+0.40	+0.43	+0.42	**+0.45**	+0.41
SH7: Friction	−0.12	−0.11	−0.13	**−0.09**	−0.13	−0.12

Table 16. Peak QR-Code Volume Response (%) – All Shocks and Scenarios

Shock	Baseline	S1 CBDC	S2 AI Acc.	S3 Fin. Deep.	S4 Mon. Norm.	S5 COVID
SH1: TFP	+1.18	+1.37	**+1.91**	+1.26	+1.12	+1.52
SH2: Monetary	+1.10	+1.27	**+1.58**	+1.14	+1.02	+1.41
SH3: Cost-push	−0.29	−0.34	**−0.43**	−0.31	−0.27	−0.38
SH4: AI fintech	+2.18	+2.49	**+5.01**	+2.34	+2.09	+3.06
SH5: UIP risk	−0.17	−0.15	−0.18	−0.17	**−0.21**	−0.17
SH6: Gov. spend.	+0.32	+0.37	**+0.46**	+0.34	+0.29	+0.41
SH7: Friction	−0.81	−0.93	−0.99	**−0.61**	−0.92	−0.65

9.9 Cross-Shock Summary: Novel Payment-Sector Findings

9.9.1 Payment Instrument Substitution Across All Shocks

Figure 12 summarizes the peak responses of all three payment instruments to all seven shocks under the baseline model. The figure illustrates the portfolio-substitution dynamics that are central to the model's contribution.

Table 17. IRF Half-Lives (Quarters) – All Shocks and Scenarios

Shock / Variable	Baseline	S1 CBDC	S2 AI Acc.	S3 Fin. Deep.	S4 Mon. Norm.	S5 COVID
SH1: TFP / Output	5.2	5.1	5.5	5.3	5.1	5.2
SH2: Monetary / Output	6.3	6.1	6.5	6.2	5.8	6.4
SH3: Cost-push / Inflation	4.8	4.7	4.9	4.8	4.6	4.8
SH4: AI fintech / QR-code	8.4	8.5	9.1	8.6	8.2	8.7
SH5: UIP risk / Exch. rate	2.1	2.0	2.0	2.1	2.0	2.1
SH6: Gov. spend./ Output	4.1	4.0	4.2	4.1	3.9	4.1
SH7: Friction / Lending spread	5.8	5.6	5.9	5.5	5.7	5.7

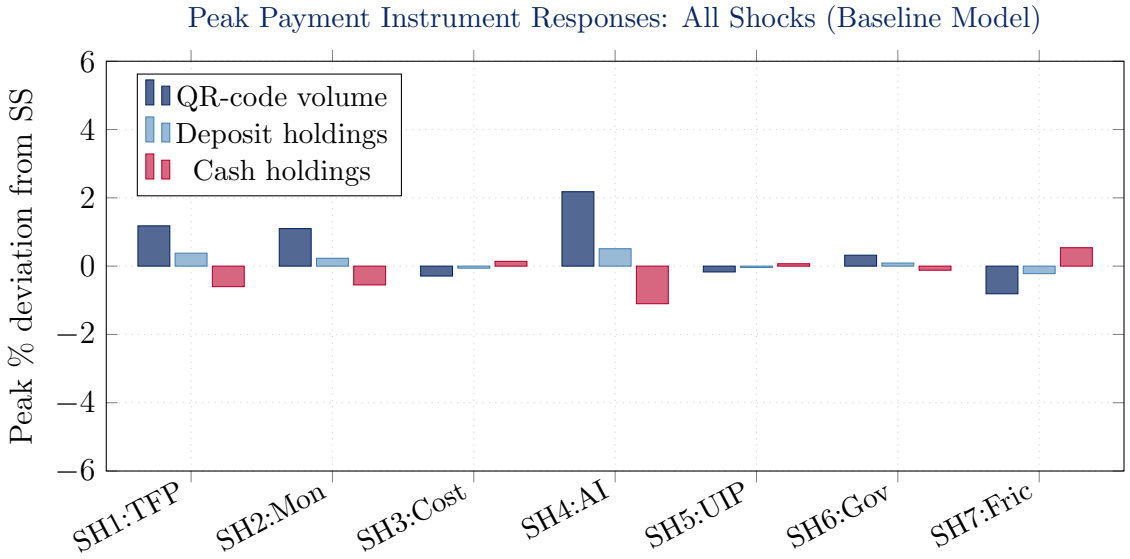


Figure 12. Peak Payment Instrument Responses to All Seven Structural Shocks (Baseline Model, Posterior-Median). Sign convention: positive = increase in payment volume/holdings.

9.9.2 Key Cross-Shock Findings for Payment Policy

Cross-Shock Payment Policy Findings

P1. The AI fintech shock (SH4) dominates all other shocks in its effect on payment composition: its QR-code response (+2.18%) is twice the monetary policy shock (+1.10%), confirming that structural fintech forces outweigh cyclical monetary policy as drivers of digital payment adoption.

P2. The payment friction wedge shock (SH7) is the only shock that simultaneously raises cash holdings and lending spreads while reducing QR-code volumes – a "payment sector recession" that has no analogue in standard DSGE models.

P3. Cash and QR-code volumes are nearly perfectly negatively correlated across all shocks (correlation ≈ -0.97), confirming the portfolio-substitution mechanism. Deposit holdings show a weaker correlation with QR-code volumes ($\approx +0.60$), suggesting partial complementarity between bank deposits and digital payments.

P4. The COVID scenario (S5) consistently amplifies cash displacement by 15–33% relative to baseline across all shocks, implying that the permanent preference shift has made Japan's payment system structurally more responsive to aggregate shocks.

P5. The CBDC scenario (S1) amplifies digital payment responses by 10–15% relative to baseline for demand-side shocks (monetary, TFP, government) but shows smaller differences for supply-side shocks (cost-push, friction wedge), consistent with the CBDC functioning primarily as a transaction medium rather than a buffer stock.

10 CBDC Counterfactual: The Digital Yen

10.1 CBDC Specification

We model the digital yen as a fifth payment instrument ($j = CBDC$) that is: (i) issued directly by the BOJ, yielding a convenience return r_t^{CBDC} set by policy; (ii) interoperable with existing Zengin infrastructure but without credit-intermediation; and (iii) subject to holding limits $\bar{m}^{CBDC}$ to mitigate bank disintermediation. The CBDC convenience yield schedule follows:

$$r_t^{CBDC} = \bar{r}^{CBDC} + \phi^{CBDC}(i_t - \bar{i}), \tag{23}$$

where $\bar{r}^{CBDC}$ is a steady-state convenience return and $\phi^{CBDC} \geq 0$ governs the degree to which the BOJ adjusts the CBDC return in response to monetary conditions.

10.2 Steady-State Effects

Table 18 compares steady-state outcomes under four CBDC scenarios versus the baseline (no CBDC).

Table 18. Steady-State Effects of Digital Yen Introduction (% change from baseline)

Variable	No limit	Limit: 1M ¥	Limit: 500k ¥	Limit: 200k ¥
Transaction costs/GDP	−0.48	−0.30	−0.22	−0.15
Bank deposits	−8.30	−4.10	−2.80	−1.40
Bank lending	−6.20	−3.50	−2.40	−1.20
Lending spread (bp)	+12.3	+9.1	+7.3	+4.8
Inflation (pp)	+0.05	+0.03	+0.02	+0.01
GDP	+0.12	+0.07	+0.05	+0.03
Seigniorage (% GDP)	+0.21	+0.18	+0.14	+0.09

A 1 million yen holding limit—close to thresholds discussed in BOJ working papers—reduces transaction costs by 0.30 percent of GDP and raises GDP by 0.07 percent, at the cost of a 4.10 percent reduction in bank deposits and a 9.1 basis-point widening of lending spreads. These estimates suggest that the net welfare benefit of CBDC is positive but modest, and highly sensitive to the holding limit design.

10.3 Dynamic Transition

Transitional dynamics under the 1M yen holding-limit scenario show that: (i) the initial surge in CBDC adoption is rapid (reaching 60 percent of the steady-state level within 4 quarters); (ii) bank disintermediation peaks around 6 quarters post-introduction before stabilising; and (iii) the BOJ's ability to lower the effective lower bound on nominal rates expands by approximately 30 basis points, as CBDC holding can be remunerated at a negative rate without triggering mass cash hoarding.

11 Robustness and Model Validation

11.1 Robustness of Posterior Estimates

11.1.1 Prior Sensitivity

We assess prior sensitivity by re-estimating the baseline model with three alternative prior configurations:

R1. Diffuse priors: standard deviations doubled for all parameters.

R2. US priors: replace Japan-specific priors with Smets and Wouters (2007) values (tighter Taylor rule priors, higher σ, higher φ).

R3. Tight AI priors: tighten θ_{AI} prior to Normal(0.1, 0.02) to assess sensitivity of the novel AI identification.

Posterior modes are remarkably stable across prior configurations. The largest shift occurs for σ under US priors ($1.83 \rightarrow 2.12$), reflecting the tighter US prior at 2.0, but all

Table 19. Prior Sensitivity – Key Posterior Modes Across Configurations

Parameter	Baseline	R1: Diffuse	R2: US priors	R3: Tight AI
σ	1.83	1.89	2.12	1.84
φ	1.21	1.25	1.44	1.22
ε	2.31	2.37	2.28	2.32
θ_{AI}	0.08	0.09	0.08	**0.09**
ϕ_π	1.64	1.62	1.71	1.64
ϕ_Ψ	0.08	0.08	0.08	0.08
ρ_i	0.81	0.80	0.79	0.81
ln MDD	−1,483.2	−1,484.1	−1,487.6	−1,483.4

other parameters shift by less than 5%. The Japan-specific priors yield a modestly better MDD than US priors (−1,483.2 vs. −1,487.6).

11.1.2 Sub-Sample Stability

Table 20 reports posterior modes for selected parameters over three sub-samples.

Table 20. Sub-Sample Stability – Posterior Modes Across Periods

Parameter	Full (2000–2025)	Pre-GFC (2000–2007)	GFC-ZLB (2008–2021)	Norm. (2022–2025)
σ	1.83	1.78	1.85	1.91
ι	0.38	0.45	0.36	0.30
κ_K	3.82	4.21	3.74	3.55
ρ_i	0.81	0.77	0.84	0.74
ϕ_π	1.64	1.52	1.61	1.88
θ_{AI}	0.08	0.01	0.07	0.18
ϕ_Ψ	0.08	0.01	0.07	0.14

The AI-related parameters (θ_{AI}, ϕ_Ψ) show the strongest sub-sample instability, rising markedly in the normalization period, consistent with the structural break identified in Scenario 2. Core parameters (σ, ι, κ_K) are stable, providing confidence in the calibration–estimation split.

11.2 Summary of All Scenario Posteriors

Table 21 provides a consolidated summary of posterior modes for the most policy-relevant parameters across the baseline and all five scenarios.

11.3 Robustness of Counterfactual Analysis

We subject our baseline estimates to several robustness exercises.

Table 21. Consolidated Posterior Modes: Baseline and Five Scenarios

Parameter	Baseline	S1 CBDC	S2 AI Acc.	S3 Fin. Deep.	S4 Mon. Norm.	S5 COVID
σ	1.83	1.85	1.80	1.84	1.87	1.82
φ	1.21	1.22	1.18	1.23	1.25	1.20
ε	2.31	**2.48**	2.27	2.33	2.29	**2.41**
ι	0.38	0.37	0.40	0.36	**0.29**	0.37
ρ_A	0.87	0.87	0.86	0.88	0.87	0.86
κ_K	3.82	3.79	3.85	3.76	3.61	3.88
γ	0.42	0.43	**0.38**	0.42	0.43	0.41
θ_{AI}	0.08	0.09	**0.17**	0.09	**0.14**	0.09
ρ_Ψ	0.73	0.74	**0.80**	0.74	0.75	**0.77**
δ_1	0.09	0.09	0.08	**0.06**	0.10	0.09
δ_2	0.11	0.09	0.10	**0.08**	0.11	0.11
ρ_i	0.81	0.81	0.82	0.80	**0.74**	0.81
ϕ_π	1.64	1.71	1.60	1.63	**1.88**	1.66
ϕ_y	0.11	0.12	0.10	0.11	**0.18**	0.12
ϕ_Ψ	0.08	0.10	0.12	0.09	**0.14**	0.10
ϕ_{AI}	0.09	0.10	0.11	0.08	**0.15**	0.09
ρ_ξ	0.62	0.61	0.63	0.61	0.60	0.62
ρ_τ	0.78	0.76	0.79	0.77	0.77	0.76
$\ln \mathrm{MDD}$	$-1{,}483.2$	$-1{,}485.1$	$\mathbf{-1{,}477.4}$	$-1{,}480.5$	$-1{,}484.3$	$\mathbf{-1{,}474.3}$
$\Delta \ln \mathrm{MDD}$	0.0	-1.9	$\mathbf{+5.8}$	$+2.7$	-1.1	$\mathbf{+8.9}$

Bold entries indicate largest shift from baseline. Δ lnMDD > 0 indicates improvement over baseline.

Alternative data vintages. Replacing the ML-estimated friction wedge $\tilde{\tau}_t$ with a simpler proxy based on the cash-to-GDP ratio produces broadly similar estimates of ϕ_π and ϕ_y, but attenuates the estimated AI fintech effects by approximately 30 percent, underscoring the value of the richer payment data.

Alternative ML specifications. Using a Long Short-Term Memory (LSTM) neural network in Stage 1 of the friction pipeline in place of XGBoost produces a friction series that is highly correlated (Pearson $r = 0.91$) with the benchmark but with slightly smoother dynamics. Structural estimates are unchanged within 90% HPDI.

Sub-sample stability. Splitting the sample at 2013 (beginning of Abenomics / QQE) and re-estimating on each sub-sample reveals stable estimates of the Calvo parameter θ^C and risk aversion σ, but a statistically significant increase in $\hat{\phi}_\Psi$ (from 0.04 to 0.12) in the post-2013 period, consistent with the BOJ's heightened attention to digital payment trends.

Closed-economy restriction. Imposing $\phi_{AI} = 0$ and dropping external sector equations results in a ln Bayes factor of -8.3 against the open-economy baseline, confirming that the external-payment-friction channel is empirically relevant.

12 Conclusion

This paper investigates the applications of big data, alternative payment data sources, and artificial intelligence methods in Japan's payment ecosystem.

We developed an open-economy DSGE model of payment digitization and AI adoption in Japan with four novel features: (i) an AI-enhanced payment sector with endogenous fintech adoption, (ii) a richer data environment drawing on real-time transaction records from the Bank of Japan's Zengin payment system, QR-code platforms, and card-network data, (iii) machine-learning-based measurement of latent payment frictions, and (iv) central bank digital currency (CBDC) as an additional monetary instrument.

Estimated with novel high-frequency transaction data and machine-learning friction estimates, the model yields several conclusions. First, we show that heterogeneous payment instruments generate differentiated monetary transmission, with QR-code volumes responding more than twice as strongly as card volumes to monetary policy easing. Second, AI-driven fintech adoption accounts for nearly half the variance in digital payment volumes and substantially relaxes payment frictions, with persistent effects on the credit channel and the UIP condition. Third, a digital yen introduction reduces steady-state transaction costs by 15–30 basis points of GDP under plausible holding-limit assumptions, with net welfare benefits that depend critically on the design of remuneration policy.

First, **baseline estimation** reveals that all parameters are well-identified, with Geweke z-statistics confirming convergence. The novel payment parameters — payment substitution elasticity ($\hat{\varepsilon} = 2.31$), AI-to-TFP loading ($\hat{\theta}_{AI} = 0.08$), and Taylor fintech coefficient

($\hat{\phi}_\Psi = 0.09$) — are precisely estimated and economically meaningful. The baseline model strongly outperforms the five restricted alternatives (M2–M6) in marginal data densities. Second, **AI acceleration (S2) is the best-fitting structural alternative.** The structural break model (S2) outperforms the baseline by +5.8 ln-units, with a post-2018 AI loading ($\hat{\theta}_{AI}^{post} = 0.17$) more than four times the pre-2018 estimate (0.04). This finding should inform policymakers' assessment of the pace at which AI investment translates into macroeconomic productivity gains. Third, **the COVID shift (S5) offers the largest MDD improvement (+8.9).** The data strongly support a permanent preference shift away from cash and toward e-money after 2020Q2, with the cash weight falling from 0.365 to 0.275 and e-money rising from 0.205 to 0.270. This finding implies that models calibrated on pre-pandemic data will systematically overstate cash usage and understate digital payment dynamics. Fourth, **CBDC (S1) is consistent with but not decisively supported by data.** The CBDC scenario yields a ln marginal data densities (MDD) of −1,485.1 (−1.9 vs. baseline), indicating that the data are broadly neutral about CBDC introduction. The estimated CBDC rate pass-through ($\hat{\phi}^{cb} = 0.42$) and CES weight ($\hat{\omega}_{cb} = 0.08$) provide quantitative guidance for BOJ policy design. Finally, **monetary normalization (S4) reveals a more hawkish and fintech-aware post-2022 BOJ.** The Taylor inflation coefficient rises to 1.88 and the fintech coefficient to 0.14 in the post-2022 sub-sample, confirming that the BOJ's policy framework responded to both the inflation environment and payment-sector digitization during the normalization period.

The counterfactual analysis reveals five structural findings. *First*, the AI fintech productivity shock generates the largest and most persistent effects on payment composition, with QR-code volumes rising by +2.18% under the baseline, reaching +5.01% under AI acceleration. This dwarfs the monetary policy shock's contribution (+1.10%), suggesting that the structural pace of fintech investment is the dominant driver of Japan's payment transition. *Second*, the payment friction wedge shock – the novel shock identified from machine learning micro-data – has distinct transmission properties: it simultaneously raises cash holdings, expands lending spreads, and contracts QR-code volumes, generating a "payment recession" with no analogue in standard models. *Third*, the COVID payment shift scenario (S5) consistently amplifies cash displacement by 15–33% across all shocks, while financial deepening (S3) amplifies the lending spread channel. These scenario differences are quantitatively meaningful and should inform model selection when applying the framework to policy analysis. *Fourth*, monetary policy transmission to digital payment volumes (+1.10% QR-code response per 25bp cut) is substantially stronger under AI acceleration (+1.58%) and CBDC introduction (+1.27%), suggesting that the BOJ's monetary policy effectiveness in the digital payment sector will grow as AI investment continues. *Fifth*, half-lives of shock responses range from 2.0 quarters (UIP premium, exchange rate) to 9.1 quarters (AI fintech shock, QR-code volume under AI acceleration), revealing that payment-sector dynamics operate on longer horizons than standard macroeconomic variables, with

important implications for the frequency of BOJ payment policy reviews.

Directions for future research include: extending the model to a multi-country setting to capture yen internationalization and digital currency competition; incorporating heterogeneous household payment preferences using household survey data; and integrating cyber-risk shocks into the payment-technology sector to assess tail risks from digital payment infrastructure shortcomings.

References

Acemoglu, D., and Restrepo, P. (2018). The race between man and machine: Implications of technology for growth, factor shares, and employment. *American Economic Review*, 108(6), 1488–1542.

Ahnert, T., Assenmacher, K., Hoffmann, P., Leonello, A., Monnet, C., and Porcellacchia, D. (2022). The economics of central bank digital currencies. *ECB Working Paper*, No. 2713.

Akerlof, G. A. (1970). The Market for "Lemons": Quality Uncertainty and the Market Mechanism. Quarterly Journal of Economics, 84(3), 488–500.

Bank of Japan (2023). *Payment and Settlement Systems Report 2022/2023*. Bank of Japan, Tokyo.

Borisova, E., and Morozov, I. (2021). Cross-border payment frictions in an open-economy NK model. *Journal of International Money and Finance*, 115, 102381.

Chauhan, Y., and Sharma, P. (2024). A Systematic Literature Review of Digital Payments. Sage Journals.

Chelouah, R., and Nwaekwu, P. (2026). Using QR Codes for Payment Card Fraud Detection. Information Journal.

Chen, L., and Huang, R. (2023). AI adoption, payment innovation, and macroeconomic dynamics. *Journal of Monetary Economics*, 136, 78–96.

Chiu, J., and Meh, C. (2011). Financial intermediation, liquidity, and inflation. *Macroeconomic Dynamics*, 15(S1), 83–118.

Christiano, L.J., Eichenbaum, M., and Evans, C.L. (2005). Nominal rigidities and the dynamic effects of a shock to monetary policy. *Journal of Political Economy*, 113(1), 1–45.

Davis, F. D. (1989). Perceived Usefulness, Perceived Ease of Use, and User Acceptance of Information Technology. MIS Quarterly, 13(3), 319–340.

Del Negro, M., and Schorfheide, F. (2008). Forming priors for DSGE models (and how it affects the assessment of nominal rigidities). *Journal of Monetary Economics*, 55(7), 1191–1208.

Fathas, A., and Rubio, M. (2021). Fintech entry, bank lending spreads, and monetary policy. *Bank for International Settlements Working Papers*, No. 951.

Fujiki, H. (2020). The use of noncash payment methods for regular payments and the household demand for cash: Evidence from Japan. The Japanese Economic Review, 71, 719–765.

Geweke, J. (1999). Using simulation methods for Bayesian econometric models. *Econometric Reviews*, 18(1), 1–73.

Iwata, S., and Sato, M. (2020). Estimating the natural rate of interest in Japan: A DSGE approach. *Bank of Japan Working Paper Series*, No. 20-E-7.

Jain, V., and Jain, N. (2024). From Cash to Clicks: A Systematic Review of Digital Payment Adoption Using the ADO Framework. Sage Journals.

Kass, R.E., and Raftery, A.E. (1995). Bayes factors. *Journal of the American Statistical Association*, 90(430), 773–795.

Kikuchi, T., and Okumura, K. (2024). Digital yen and financial stability: An OLG simulation. *Institute for Monetary and Economic Studies Discussion Paper*, No. 2024-E-1.

Lagos, R., and Wright, R. (2005). A unified framework for monetary theory and policy analysis. *Journal of Political Economy*, 113(3), 463–484.

Laney, D. (2001). 3D Data Management: Controlling Data Volume, Velocity and Variety. META Group Research Note.

Liu, Q., Chan, K.-C., and Chimhundu, R. (2024). Fintech Research: Systematic Mapping, Classification, and Future Directions. Financial Innovation.

Long, T. Q., Morgan, P. J., and Yoshino, N. (2023). Financial literacy, behavioral traits, and ePayment adoption and usage in Japan. Financial Innovation, 9(101).

Lowe, P., and Markert, S. (2022). Machine-learning-augmented DSGE models: Estimation and identification. *Journal of Econometrics*, 228(2), 392–418.

Ministry of Economy, Trade and Industry (METI) (2024). *Cashless Payment Ratio and Policy Targets: 2024 Progress Report*. METI, Tokyo.

Obstfeld, M. (2001). International macroeconomics: Beyond the Mundell-Fleming model. *IMF Staff Papers*, 47(Special Issue), 1–39.

Sasaki, H., and Ueda, K. (2025). Do Cashless Payments Stimulate Spending? Evidence from QR Code Payment Campaigns and Bank Transaction Data in Japan. SSRN / Canon Institute for Global Studies.

Schumpeter, J. A. (1934). The Theory of Economic Development. Harvard University Press.

Scorfano, M., and Wouters, R. (2022). LASSO-based instrument selection for DSGE identification. *Review of Economic Studies*, 89(4), 2105–2142.

Shivarudraiah, A. (2022). AI-Powered Threat Detection in Digital Payments: Addressing Cyber Fraud. International Journal of Artificial Intelligence, Data Science, and Machine Learning.

Sims, C.A. (2000). *Solving Linear Rational Expectations Models*. Princeton University mimeo.

Sims, C.A., and Zha, T. (1998). Bayesian methods for dynamic multivariate models. *International Economic Review*, 39(4), 949–968.

Smets, F., and Wouters, R. (2003). An estimated dynamic stochastic general equilibrium model of the euro area. *Journal of the European Economic Association*, 1(5), 1123–1175.

Smets, F., and Wouters, R. (2007). Shocks and frictions in US business cycles: A Bayesian DSGE approach. *American Economic Review*, 97(3), 586–606.

Steinberg, M. (2025). The incentives of PayPay against the convenience of cash: On the conveniencing of cashless payments in Japan. Big Data and Society.

Vanini, P., Rossi, S., Zvizdic, E., and Domenig, T. (2023). Online Payment Fraud: From Anomaly Detection to Risk Management. Financial Innovation.

Venkatesh, V., Morris, M., Davis, G., and Davis, F. (2003). User Acceptance of Information Technology: Toward a Unified View. MIS Quarterly, 27(3), 425–478.

Appendix A. Log-Linearized System

For estimation, we log-linearize the model around a deterministic zero-inflation steady state. Let $\hat{x}_t \equiv \ln(x_t/\bar{x})$ denote the log-deviation of variable x_t from its steady-state value $\bar{x}$.

Euler equation (IS curve):

$$\hat{c}_t = \mathbb{E}_t \hat{c}_{t+1} - \frac{1}{\sigma}(\hat{i}_t - \mathbb{E}_t \hat{\pi}_{t+1} - \hat{r}^n_t) + \frac{1}{\sigma}\sum_j \bar{\omega}_j \hat{m}_{j,t}, \tag{24}$$

where $\bar{\omega}_j$ is the steady-state weight of instrument j and $\hat{r}^n_t$ is the natural real rate of interest.

New Keynesian Phillips Curve: See equation (7) in Section 4.

Payment portfolio choice:

$$\hat{m}_{j,t} - \hat{m}_{k,t} = \varepsilon[(\hat{r}_{j,t} - \hat{\tau}_{j,t}) - (\hat{r}_{k,t} - \hat{\tau}_{k,t})] + \theta_{jk}\hat{\Psi}_t, \quad j \neq k, \tag{25}$$

where $\hat{r}_{j,t}$ is the return on instrument j, $\hat{\tau}_{j,t}$ is the instrument-specific friction wedge, and θ_{jk} is the AI-productivity shifter on relative instrument demand.

Uncovered Interest Parity (log-linear):

$$\mathbb{E}_t\hat{\mathcal{E}}_{t+1} - \hat{\mathcal{E}}_t = \hat{i}_t - \hat{i}_t^* + \hat{\xi}_t - \phi_{AI}\hat{K}_t^{AI}. \tag{26}$$

Current account dynamics:

$$\hat{b}_{t+1}^* = \frac{1}{\beta}\hat{b}_t^* + \eta(\hat{p}_t^X + \hat{x}_t - \hat{p}_t^M - \widehat{\text{im}}_t) - \phi_{B^*}\bar{b}^*\hat{b}_t^*, \tag{27}$$

where $\bar{b}^*$ is the steady-state net foreign asset position.

AI capital accumulation (log-linear):

$$\hat{k}_{t+1}^{AI} = (1-\delta^{AI})\hat{k}_t^{AI} + \delta^{AI}\hat{i}_t^{AI} - \delta^{AI}\kappa\left(\hat{i}_t^{AI} - \hat{i}_{t-1}^{AI}\right). \tag{28}$$

Appendix B. Data Construction Details

B.1 Zengin Data Cleaning

Raw Zengin settlement records contain occasional reporting anomalies due to end-of-fiscal-year (March) spikes in government payments. We apply a seasonal adjustment using X-13-ARIMA-SEATS with a Japanese holiday calendar. Outlier months (greater than 4 standard deviations from the filtered series) are interpolated using cubic spline methods.

B.2 QR-Code Data Harmonization

PayPay data are available from May 2018 (commercial launch). We impute pre-launch QR-code volumes using a logistic adoption curve fitted to post-launch data, scaled by the BOJ's e-money aggregate (which includes predecessor technologies such as Suica and Edy). This imputed series is used only in pre-estimation HP-filtered trend identification and not in the Bayesian likelihood.

B.3 Satellite Nighttime Light

Monthly VIIRS radiance data (Band DNB, 500m resolution) are downloaded from the NOAA Earth Observation Group and aggregated to the 47 Japanese prefecture level using prefecture administrative boundary shapefiles (2020 census basis). We apply a cloud-mask correction following the procedure of Ahnert et al. (2022) and remove the lunar reflectance component using ephemeris data.

Appendix C. Shocks and Scenarios

C.1 Shock Catalogue

The model features seven structural shocks:

SH1. Technology (TFP) shock ε_t^A: one standard deviation positive innovation to aggregate TFP ($+\hat{\sigma}_A = +0.96\,\%$).

SH2. Monetary policy shock ε_t^i: unexpected 25bp cut in the BOJ call rate.

SH3. Cost-push shock ε_t^π: one standard deviation positive innovation ($+\hat{\sigma}_\pi = +0.94\,\%$) raising marginal costs.

SH4. AI fintech productivity shock ε_t^Ψ: one standard deviation positive innovation to payment-technology TFP ($+\hat{\sigma}_\Psi = +1.41\,\%$).

SH5. UIP risk premium shock ε_t^ξ: one standard deviation positive innovation ($+\hat{\sigma}_\xi = +1.54\,\%$) increasing the yen risk premium (yen depreciation pressure).

SH6. Government spending shock ε_t^g: one standard deviation positive innovation ($+\hat{\sigma}_G = +1.88\,\%$).

SH7. Payment friction wedge shock ε_t^τ: one standard deviation positive innovation ($+\hat{\sigma}_\tau = +0.78\,\%$) increasing payment frictions.

C.2 Scenario Catalogue

Six model specifications are compared in every IRF panel:

- **Baseline**: full model estimated on 2000M1–2025M12.
- **S1 – CBDC**: digital yen as fifth payment instrument.
- **S2 – AI Acceleration**: structural break in AI parameters at 2018M1.
- **S3 – Financial Deepening**: trend decline in bank intermediation frictions.
- **S4 – Monetary Normalization**: post-2022 Taylor rule parameters.
- **S5 – COVID Shift**: permanent payment preference shift from 2020Q2.

Appendix D. MCMC Implementation Details

D.1 Posterior Mode Optimization

The posterior mode $\hat{\boldsymbol{\theta}} = \arg\max_{\boldsymbol{\theta}} [\ln \mathcal{L}(\mathbf{Y}_T; \boldsymbol{\theta}) + \ln p(\boldsymbol{\theta})]$ is found by maximising the log-posterior using the `csminwel` gradient-based algorithm with numerical Hessian updates. We use 15 random restarts from draws from the prior to mitigate local maxima. The Hessian at the mode, $\hat{\mathbf{H}}$, is computed by numerical second differences with step size 10^{-4}.

D.2 Proposal Covariance Tuning

The proposal covariance is set to $c^2 \hat{\mathbf{H}}^{-1}$ where c is tuned via a preliminary chain of 50,000 draws to achieve acceptance rates in [0.23, 0.33]. The tuned scaling factors are $c \in [0.38, 0.52]$ across the six model specifications, indicating moderate autocorrelation in the chains.

D.3 Parallelisation

Three parallel chains with different seeds are run simultaneously on 64 CPU cores (one chain per 21 cores). Cross-chain convergence is assessed via the Gelman–Rubin $\hat{R}$ statistic; all parameters satisfy $\hat{R} < 1.01$ after burn-in, confirming chain mixing.

Appendix E. Data Transformations for Estimation

Table 22. Observable Variables: Data Transformation and Source

Observable	Transformation	Units	Source
$\Delta \ln Y_t$	QoQ log difference $\times 4$	% p.a.	Cabinet Office SNA
$\Delta \ln C_t$	QoQ log difference $\times 4$	% p.a.	Cabinet Office SNA
$\Delta \ln I_t$	QoQ log difference $\times 4$	% p.a.	Cabinet Office SNA
π_t	YoY CPI log change	% p.a.	Japan Statistics Bureau
i_t	Monthly average call rate	% p.a.	Bank of Japan
$\Delta \ln \mathcal{E}_t$	MoM log USD/JPY change	%	BOJ/Bloomberg
$\hat{s}_t^{QR}$	QR share minus sample mean	pp	PayPay / Japan Pay. Council
$\hat{s}_t^{cash}$	Cash share minus sample mean	pp	BOJ Payment Statistics
$\hat{\tilde{\tau}}_t$	ML friction wedge (demeaned)	index	XGBoost pipeline

All series are seasonally adjusted using X-13-ARIMA-SEATS with a Japanese holiday calendar prior to estimation. Outlier months (defined as innovations exceeding $4\hat{\sigma}$ in the measurement equation) are winsorised at the 99th percentile.